Multifinger Caliper Interpretation and Applications

Nicolas Kotlar

1. Introduction

Multifinger Calipers were introduced in the 1950s and still remain one of the most popular measurements for casing and tubing monitoring. Even though there have been many advances in the electronics, materials and mechanical design, the working principle is the same.

Multifinger calipers are downhole inspection tools, where a number of fingers record the internal surface of the pipe. A continuous log of the pipe's internal diameter can allow us to quantify the metal loss due to corrosion or erosion, caused by the nature of the downhole environments. As the pipe loses metal and the wall thickness decreases, the necessary mechanical properties to withstand the internal and external pressures and stresses can be compromised. On the other hand, deposition of salts, carbonates, hydrates, etc., may reduce the pipe diameter, impacting on the well productivity due to increased pressure losses. For extreme cases of deposition, it may not be possible to pass through the restriction, which will prevent future well intervention activities. When the earth stresses are enough to change the trajectory of the pipe, deformation will occur, which can also complicate the well entry activities, and represents an integrity risk as well. MFC can be used to diagnose the following conditions, among others:

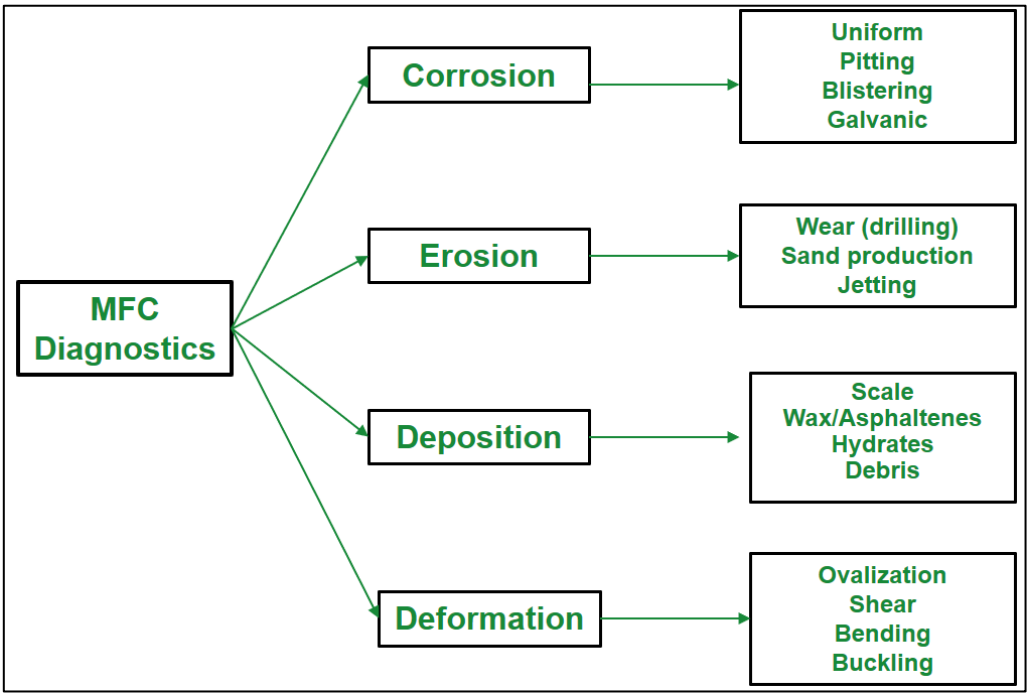

Fig. 1 – MFC Applications

This document intends to provide an introduction to Multifinger Caliper interpretation and their main applications. A number of Frequently Asked Questions (FAQs) on common topics are answered in the different sections. The last section offers a brief introduction to pipe integrity evaluation through ultrasonic pulse-echo tools.

2. Multifinger Caliper tools

Multifinger Caliper (MFC) tools contain an array of arms or 'fingers', which measure independently the radius from the centre of the tool, to the pipe wall. After processing, these radii readings will provide a map of the internal pipe condition, allowing to identify different features like penetration, deposition, deformation, etc.

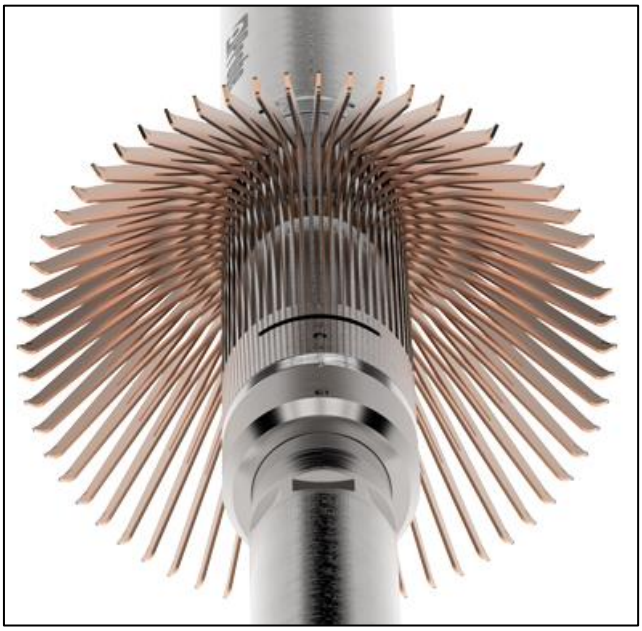

Fig. 2 – 60 finger Caliper – Courtesy: Probe - ProMAC™

This family of tools come with different number of fingers to suit various pipe sizes. The most typical configurations are listed below:

Fingers	Tool OD (in)	Maximum measurable Pipe ID (in)
24	1 11/16	4.5 (7'' extended fingers)
40	2 ¾	7 (10'' extended fingers)
60	3.9 - 4	10 (13 - 14'' extended fingers)

Extended finger can be fitted in order to increase the maximum finger opening. Other MFC tools come with 56 or 80 fingers.

The quoted fingers radial resolution is around 0.001 – 0.004 in, for standard fingers (not extended). The radial accuracy is about +/- 0.02 – 0.04 in. These metrology characteristics make the tool very sensitive to ID changes. For example, for a 7 in, 29 lb/ft (nominal pipe thickness of 0.408 in) it would be possible to distinguish penetration variations of ~0.6%.

These tools are designed to measure only during up passes. Also, in order to achieve a good vertical resolution, the standard logging speeds are ~ 30 ft/min (10 m/min). The vertical resolution is of course a function of the data transition (telemetry rate) as well, but at the typical logging speeds it is common to have 100 samples per foot for this type of measurements. Compared to Production Logging, where a 2 samples per foot is used, and where only a particular range of the well is logged, the data file size of MFC acquisitions is, in general, much larger.

While running in hole, the tool fingers are closed. Only when reaching the target depth, the fingers are opened using a motor, which drives a lead screw, providing the linear motion to open and close the fingers. This can be done both in real time (wireline operations) and through memory commands.

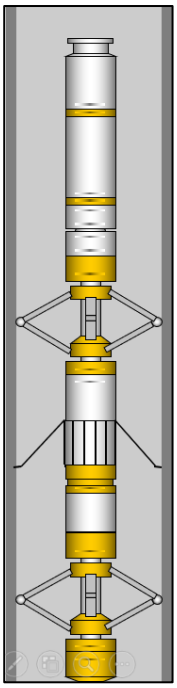

Fig. 3 – MFC toolstring schematic

For achieving this level of radial accuracy and resolution, it is critical that the MFC tool is properly centralized. We will see in Section 3 what the effect of the tool eccentricity is. Strong mechanical centralizers are typically set above and below the MFC.

The MFC deployment typically includes setting knuckle joint, with the objective to decouple the measurement section from the momentum created by the conveyance method and possible weight bars. Also, swivel joints can help to avoid excessive tool rotation.

Modern MFC tools include a relative bearing measurement, which will allow us to orient the different internal features found during the survey. Apart from the MFC, depth control measurements (CCL, GR) are added. Also, depending on the objectives of the survey, temperature, pressure, spinner and noise sensors can also complement the MFC measurements.

FAQ 1: What is the circumferential resolution of the MFC measurements?

We will see in this section the main characteristics of the fingers, but at this stage it is necessary to know that the finger width that makes contact with the pipe is about 0.063 in (1.6 mm). Therefore, for an *n* fingers caliper, we can say that the surveyed perimeter of the pipe is *n*0.063 in.*

The nominal internal perimeter of the pipe is π*ID. So if we take a 7 in, 29 lb/ft pipe (6.184 in), the nominal pipe perimeter is 19.42 in.

So what percentage of the pipe will be covered? If we use a 40 fingers caliper, then we'll get:

$$\%Covered = \frac{0.063 * 40}{\pi * 6.184} * 100 \cong 13\%$$

This calculation can give us an idea of the data we may be missing. In general, this will not impact on the detection of deformation, homogeneous deposition/metal loss or ovalization, but we can for sure miss some pitting and small holes.

In general:

$$\%Covered = \frac{finger\ tip\ width * number\ of\ fingers}{\pi * nominal\ ID} * 100$$

MFC fingers

Once at target depth, the fingers will open and (hopefully) make contact with the pipe inner wall. Each finger assembly is independent, and contains a number of elements as shown in the image below:

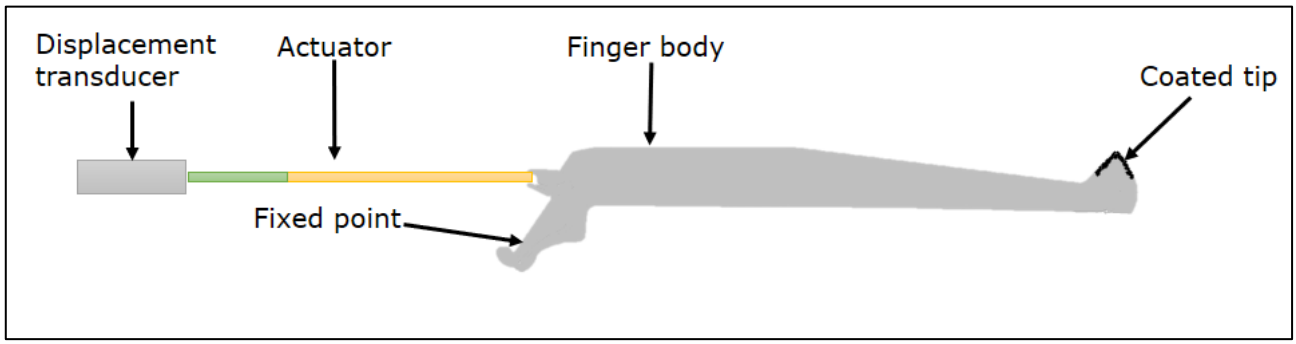

Fig. 4 – Finger assembly

- Finger body: made of a bendy material (low Young modulus) that can withstand fatigue (i.e. Beryllium copper). Depending on the design, the finger body may contain a spring that pushes the finger open. The fingers exert a contact force (~ 1lbf) on the pipe.
- The tip of the finger will be scratching the internal surface of the pipe for thousands of feet, and therefore is coated with a hard, abrasive material, such as Tungsten carbide. The fingers are re-coted after certain number of feet of logging (i.e. 40-60k ft).
- The Fixed point or Pivot: This part of the finger is inside the tool housing (not visible when the tool is assembled). This part does not allow lateral or vertical movement, only angular rotation.
- Actuator: A magnetic actuator rod is connected to the finger. As the finger opens and closes, the actuator will move horizontally.
- Displacement transducer: typically uses LVDT (Linear variable displacement transducer) or DVRT (Differential variable Reluctance Transducer). Both types of transducers contain coils that as the actuator moves in and out, the inductance changes, allowing to measure the displacement of the rod. This will be associated with a finger opening.

The image below shows the principle of measurement. The angular position of the finger changes as it senses pipe ID variations. This angle, and therefore the finger radius measurement is related to the transducer measurement, as the actuator moves in and out the coils.

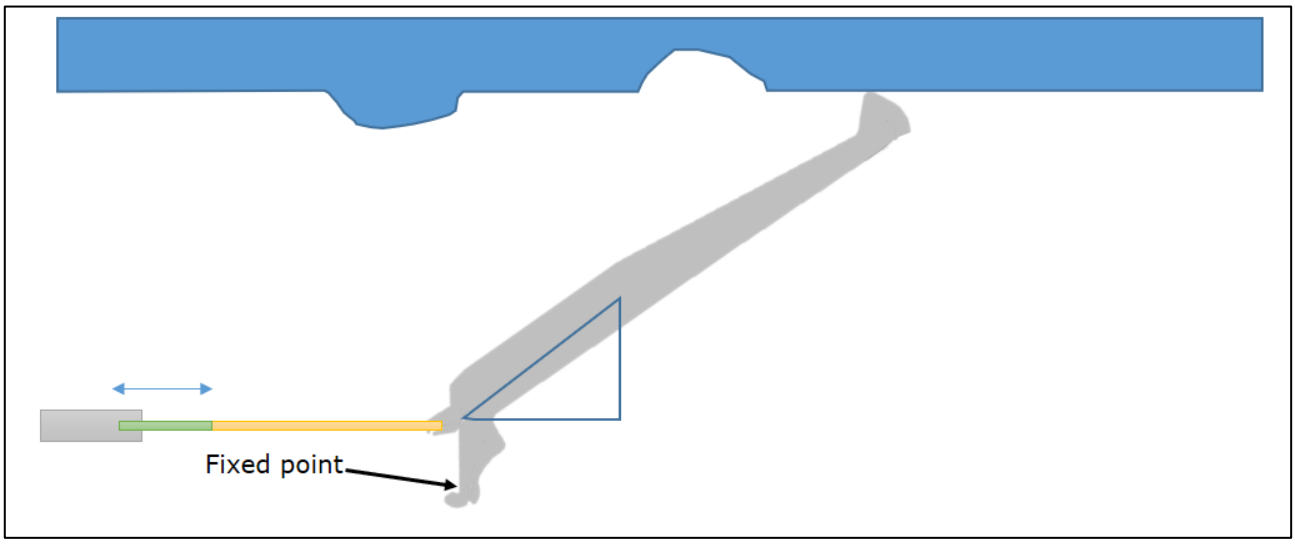

Fig. 5 – Finger movement

Fingers surface calibration

Relating the transducer's electrical signal to the radius measurements is achieved through a surface calibration process. As explained above, the actuator position is a function of the angular movement of the finger. But also the temperature will play an important role, as materials suffer of expansion, the electrical response changes, etc. Different tool manufacturers and service companies follow different guidelines in terms of the best way to perform these calibrations.

The first calibration type is done at room temperature, and consists on running the MFC tool through a number of calibrated rings. The sensor's electrical response is measured and plotted vs. ring size. In general, a pre and post job calibration should be performed, and these should include the pipe sizes to be logged during the job.

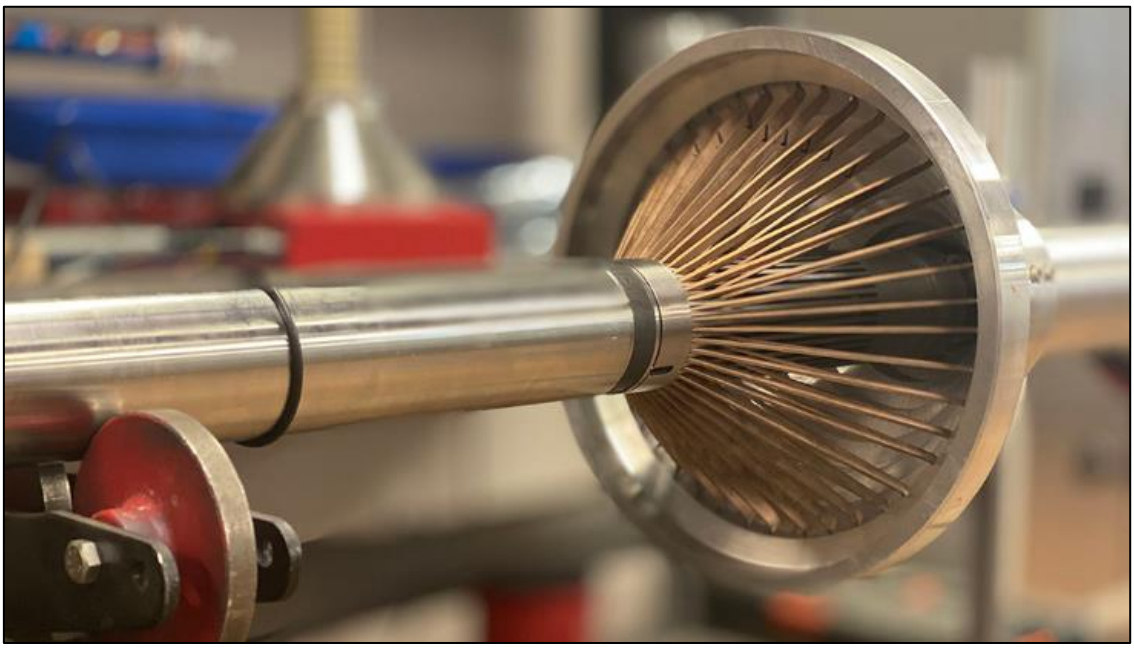

Fig. 6 – Fingers surface calibration - Courtesy: Probe

The second calibration type is also known as 'Temperature compensation'. The tool is put inside an industrial oven, and is subjected to temperature variations, typically increasing steps. There may be a number (i.e. 8) of rings of different diameters. This type of calibration is not performed as often as the first type.

The results of these calibrations are several files that are loaded into the acquisition system in order to convert the electrical response into a radius value. The plots below show the typical shape of these calibrations.

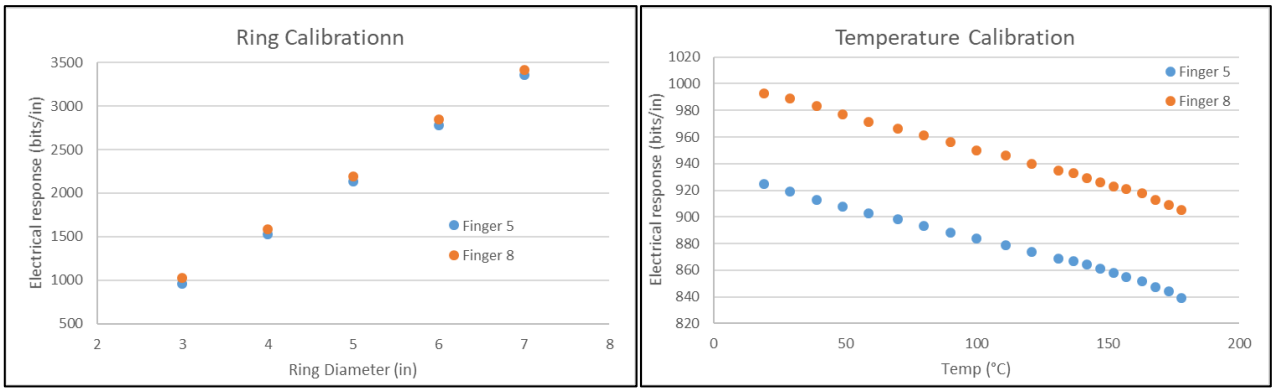

Fig. 7 – Fingers ring calibration at room temperature (left) and temperature compensation at constant ring size (right)

3. MFC Processing

In this section we will explore the processing options to go from raw MFC data to the stage where meaningful statistics can be extracted from it. The starting point for the MFC processing is, in general, a file which contains one radii value for each finger, without any other further processing applied by the acquisition system, apart from the calibration and temperature compensation.

As with any other cased hole log, telemetry or electronic noise may be present, which in many cases may be solved by applying an adequate filter. Also, malfunctioning arms should be removed, and its value should be replaced by some statistic or average of the neighboring arms.

MFC tools contain an even value of arms, and sometimes the acquisition system allows the export of the computed diameters based on the sum of opposite arms. For reasons that we will explain below, it is recommended to always start from raw fingers radii values.

3.1. Centralization

Figure 3 shows the schematic of an MFC tool, which is perfectly concentric with the pipe. Even though the tool is run with centralizers and knuckle joints are normally used, the tool will be eccentric. MFC are in general heavier than production logging sensors, and sometimes these are run in tandem with other heavy modules, like cement tools. Even for low deviations (i.e. 5 deg), the toolstring will move from the centre as shown in Figure 8.

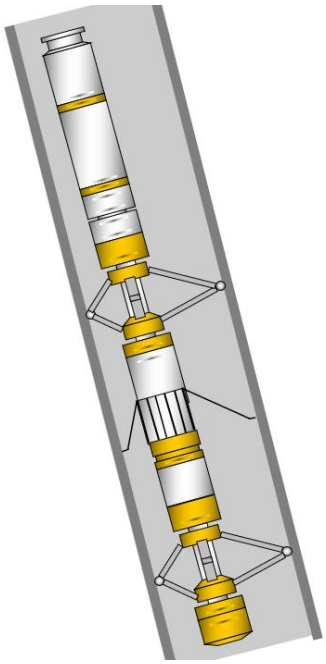

Fig. 8 – MFC toolstring schematic

A cross-sectional image of the ideal centralized case (Figure 3) and eccentric MFC (Figure 8) are shown in the image below. For a 16 finger MFC, with finger 1 pointing up (0 deg) and finger 9 pointing down (180 deg). The radii as measured for each finger is shown in blue (perfectly centralized) and in black (eccentric).

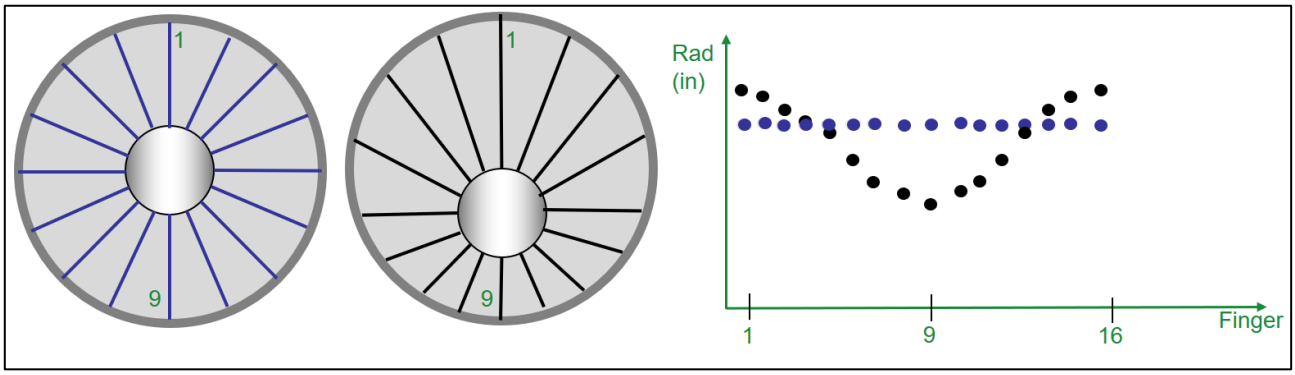

Fig. 9 – MFC toolstring schematic

In the case of a perfectly centralized MFC, the measured radii can be used directly in order to obtain the diameters and statistics (penetration, reduction, etc.). For a pipe in perfect condition, the radii as measured by each finger should be the same.

For the eccentric pipe, gravity pushes the centre of the MFC down. Finger 1 now is more open than finger 9, and the radii distribution resembles that of a sinusoid. It is clear that these radii readings cannot be used directly to compute the statistics.

Different automatic tracks generated by Emeraude can be used for identifying eccentricity and assessing the need of centralization. The image below shows a 10000 ft long pipe, with deviation going from 0 to 75 deg.

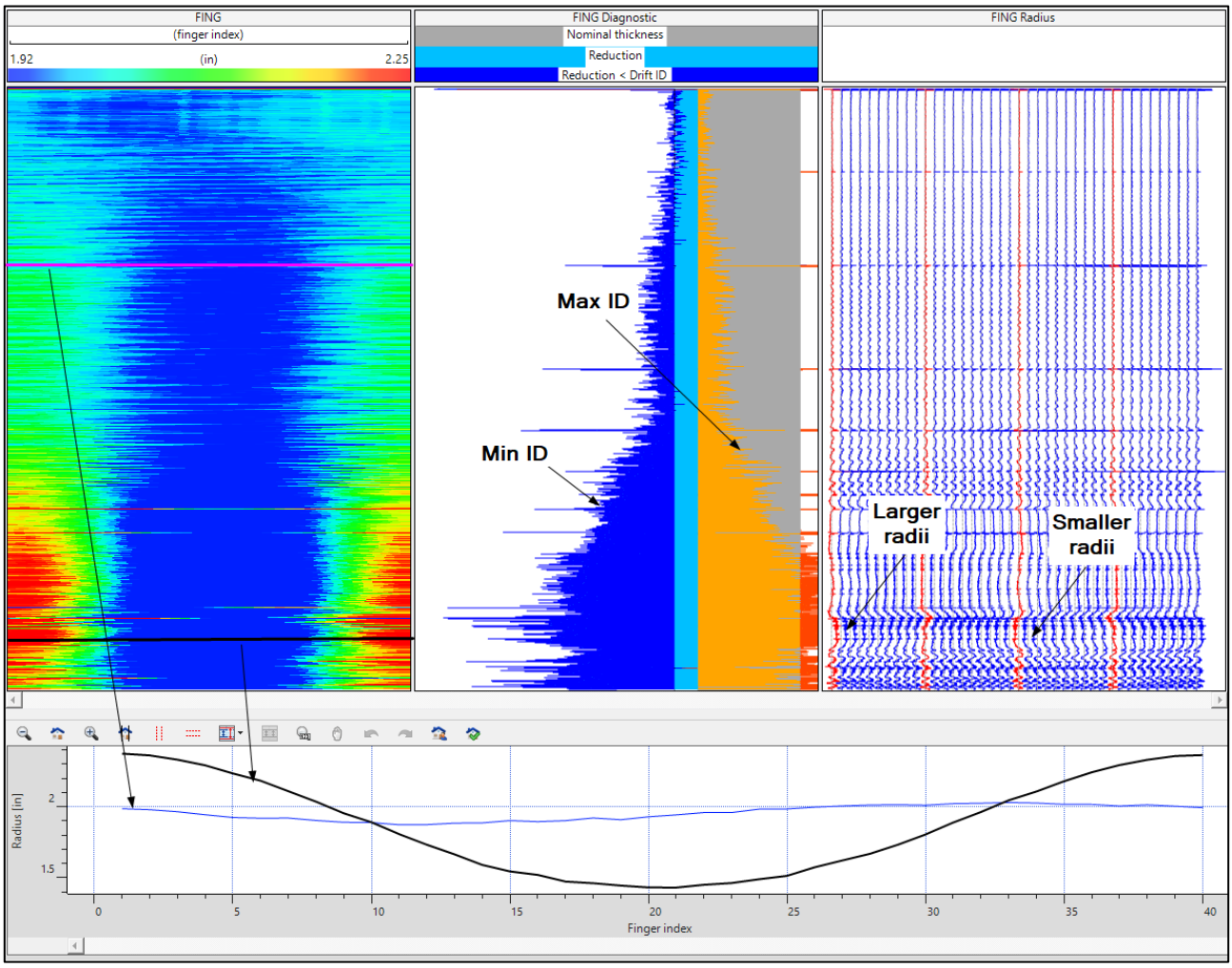

Fig. 10 – Diagnostic plots for eccentricity

- The MFC image corrected for bearing shows that in the low side of the pipe (centre of the image) the radii measurements are smaller than on the high side of the pipe. This difference gets more pronounced with depth, as the deviation increases.
- The MFC Diagnostic plot show large differences between Maximum and Minimum ID, and again this difference increases with deviation.
- The Radius track shows that some of the fingers measure higher than the nominal radius, while others measure below nominal.
- The Radius vs. finger view shows that the radii distribution for two different depths, in blue at a shallower depth and in black at a deeper depth. The sinusoidal shape is present in both cases, even though at a deeper depth the amplitude is higher due to the larger contrast between Min and Max Radii.

Finally, the cross-section image overlaps the nominal pipe geometry with the actual measurements. In red, the fingers measurements are displayed, which show that indeed the arms sense a circular shape, but this is displaced with respect of the nominal pipe.

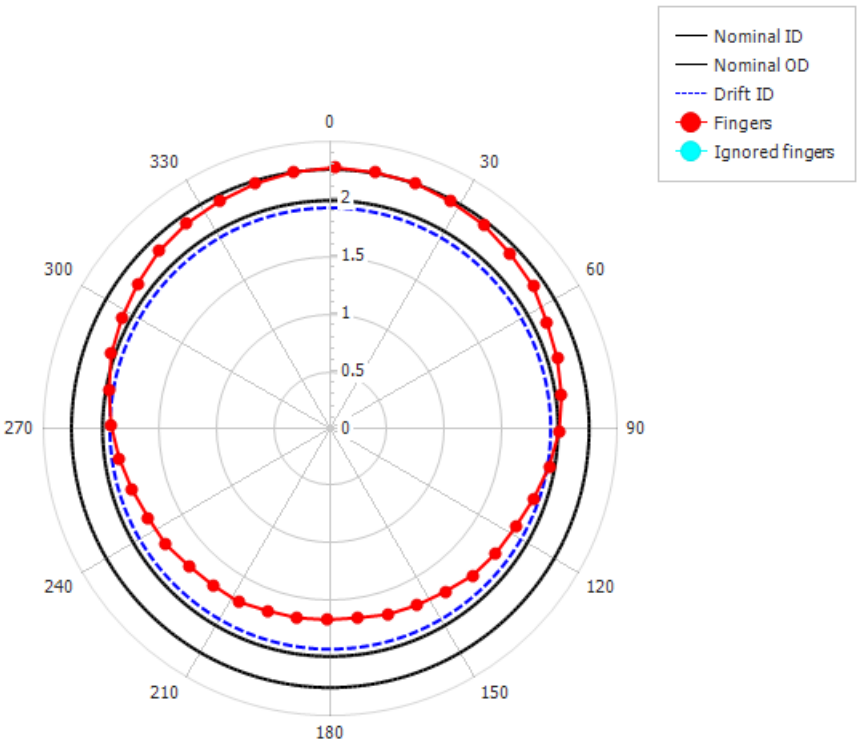

Fig. 11 – Eccentric cross-section

All these diagnostic plots help to understand the need of centralization.

The fingers measurements are given in cylindrical coordinates, this is a radius, an angle and a depth. For every row of depth, we can locate the radius measurements on a Cartesian coordinate system, using sine and cosine relationships. The image below shows a case of a circular pipe in perfect internal condition.

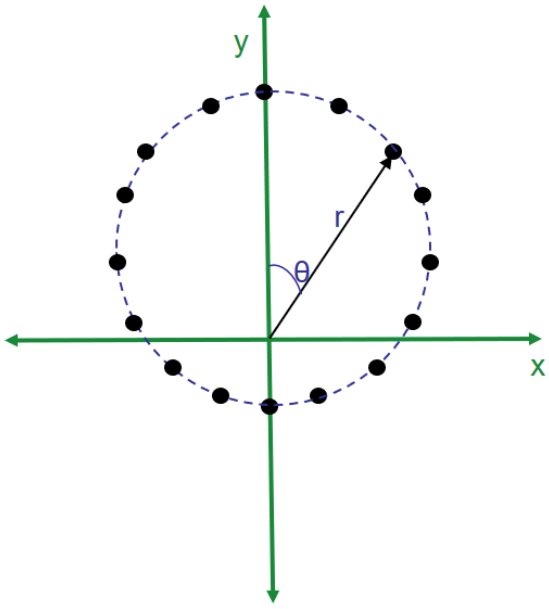

Fig. 12 – Radii measurements in a Cartesian plane

The first part of the centralization consists on fitting a shape to the measured points. The simplest approach is to use the equation of an eccentric circle:

$$R^2 = (x - x_c)^2 + (y - y_c)^2$$

Where x_c and y_c are the coordinates of the actual centre of the pipe.

However, due to stresses in the formation or induced by the manufacturing process, the pipe may be ovalized. In this case, an ellipse shape would fit better the measured points. The equation of the eccentric ellipse is

$$1 = \frac{(x - x_c)^2}{a^2} + \frac{(y - y_c)^2}{b^2}$$

Where *a* and *b* are the semi-minor and semi-major axis of the ellipse. The actual equation used in Emeraude also takes into account the ellipse orientation, as in the formula presented above, the axes are orthogonal with x and y. Note that when *a=b=r*, we are back to the equation of the eccentric circle. Therefore, the ellipse equation is a more generic solution, and is used by default in Emeraude, unless the user explicitly selects circular fitting.

The second part of the centralization is basically a transformation of coordinates. Once the actual centre of the pipe was determined, the radii and angle of each finger is recomputed, again using the Euclidian distance approach:

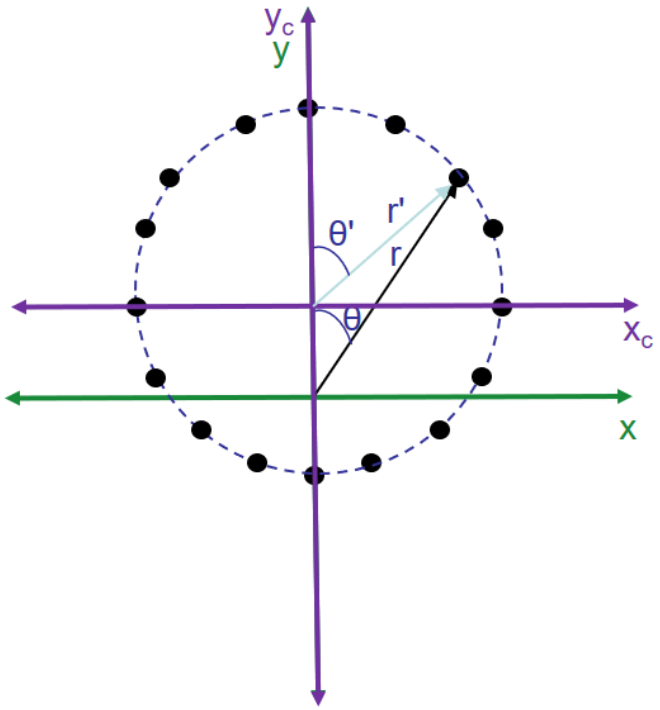

Fig. 13 – Recomputed radii after centralization.

So far the explanation has considered perfect internal pipe condition. In reality, the caliper is likely to find a number of penetrating or depositional features that will impact on the shape of the pipe. Let's imagine that the drilling bit left a grove that is sensed by two fingers, as shown in yellow in the image below. As the shape of the ellipse (or circle) is computed using non-linear

regression, by using all the fingers, including the ones that 'feel' the grove and are not part of the perfect shape, the estimated centre will be shifted. However, by excluding the two measurements in yellow, it would be possible to obtain the centre of the 'unaffected' part of the pipe.

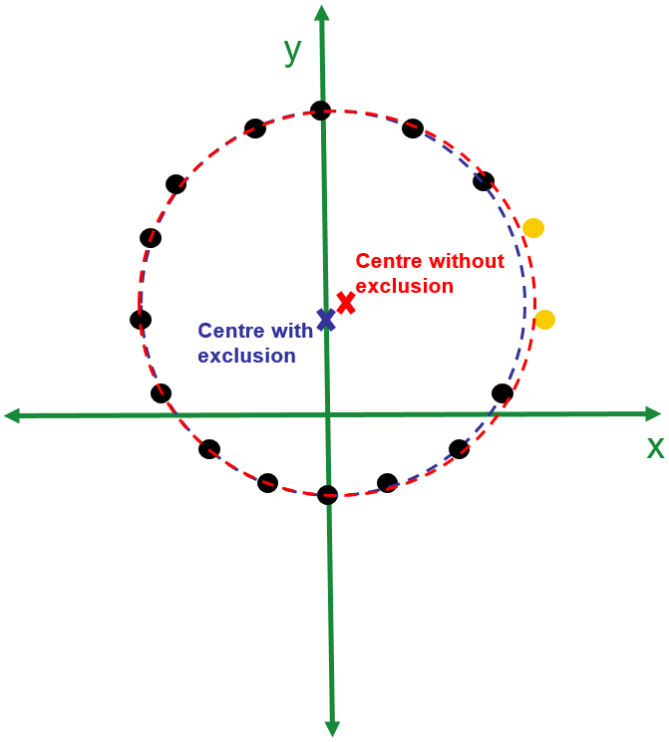

Fig. 14 – Fingers exclusion.

Emeraude offers a number of exclusion options, which are based on the distance of the finger's measurement to the one of the fitted shape. The user may decide to exclude *n* fingers that maximize the distance above (Maximum), below (Minimum) or both (Absolute) compared to the fitted ellipse or circle. Also, it is possible to base the exclusion on the percentage variation of radii of consecutive arms.

Once the centralization is applied using certain exclusion criteria, Emeraude will display the excluded arms in blue in the cross section image, as shown below. For example, three of the excluded arms correspond to a penetrating feature, and it is indeed correct to remove them from the fitting. However, there is one isolated point that was removed based on the exclusion criteria (in this case, maximum absolute distance), which should not necessarily be removed. In this case, there are still 36 valid finger values for the fitting. However, as with any non-linear regression, unnecessary over-excluding measurements can impact negatively on the quality of the fitting. The interpreter must navigate through the raw dataset, understanding the nature and distribution of the penetrating and depositional features, and apply the centralization accordingly. It is possible to apply different exclusion criteria for the different depths.

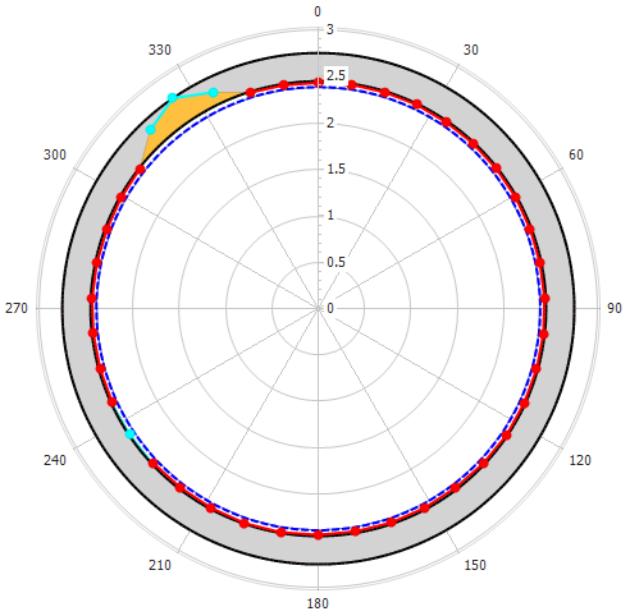

Fig. 15 – Excluded fingers in the Cross-section image

Once the centralization is completed, the Eccentricity will be calculated, as the difference between the centre of the pipe and the centre of the MFC tool. Also the regression residual expressed as chi-square ($1-R^2$) is displayed.

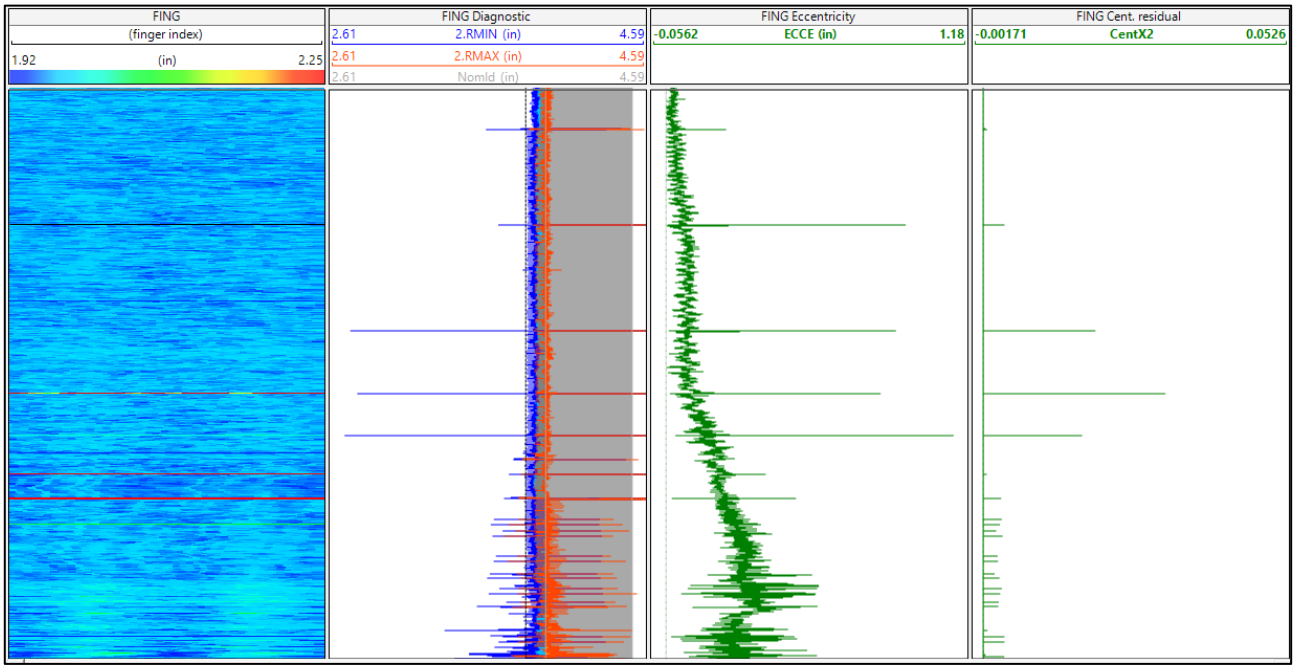

Fig. 16 – Centralization results

Spikes on the residual should get the interpreters attention as they are indication that the fit is less satisfactory in certain intervals. For example, the log shown in Figure 16 was centralized

using an ellipse fit, excluding the 4 fingers with larger absolute difference. The spikes seen in the residual (also in the eccentricity) correspond to valves, SSDs and side pocket mandrels. Looking at one of the SPMs, it can be seen that 8 arms are actually affected by the presence of the increased diameter. When trying to fit these shapes, only excluding the 4 arms of larger absolute distance, Emeraude uses an ellipse displayed in purple in the image below (on the left). The four arms that were excluded are indeed the correct ones, but not the only ones that should have been removed from the fitting. A local centralization excluding 8 arms was applied (image on the right) and in this way the SPM can be fitted pretty much by a perfect circle:

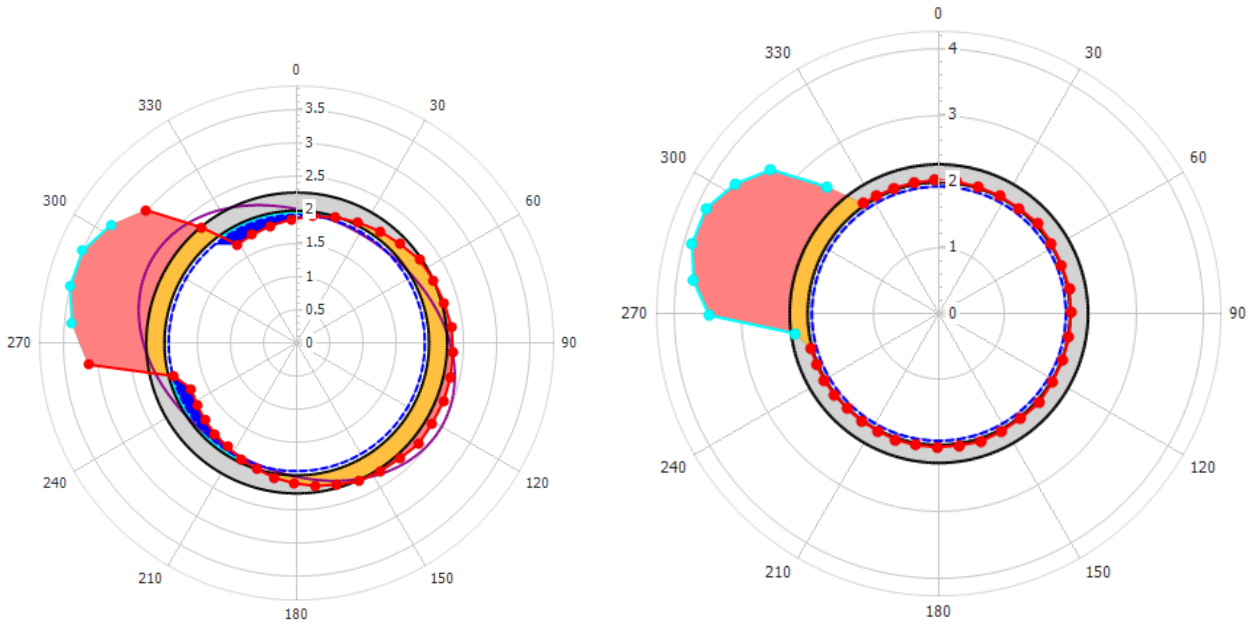

Fig. 17 – Excluded fingers in the Cross-section image

These types of completion elements do not represent the nominal pipe joints, however through this example it can be seen the importance of understanding the settings of the centralization.

FAQ 2: What is the maximum eccentricity that your centralization algorithm can handle?

This question comes from the heritage of older centralization algorithms, which used a 1D fitting (i.e. sinusoidal). As can be concluded from the explanation above, as long as we are able to accurately locate the fingers measurements on a Cartesian coordinate system, then there are no restrictions on the level of eccentricity from the algorithm point of view.

So the question should be, does the eccentricity affect the accuracy or resolution of the fingers measurements?

And the answer is yes. The finger's resolution is given by the possibility of quantifying the actuator displacement, which in turn is driven by the angular movement of the finger. For an eccentric MFC, the fingers on the side of the short radius measurements will experience a much smaller angular movement, meaning that the actuator displacement will also be smaller. This, in essence is same principle why extended fingers reduce the radial resolution compared to the standard finger in a pipe where both fingers types are suitable.

FAQ 3: Can the centralization 'deform' the pipe shape?

This question is typically asked based on the fact that the fitting uses an ellipse or a circular fitting.

The answer is that the centralization will not deform the fingers measurements. Again, the fitting provides the centre of the ideal shape, and then the fingers radii are recomputed, but using the actual MFC measurements. Therefore, the shape will not be modified: if the pipe is ovalized, if there are penetrating/depositional features, they will be there before and after the centralization. However, as shown in Figure 16, a wrong estimation of the geometrical centre by the fitting will be reflected as a translation of the fingers measurements. This will indeed have consequences, as the distance to the maximum or minimum radius measurements will change, which in turn will affect the calculations of penetration, reduction, etc. However, again, the shape of the pipe is not modified, just displaced.

In situations like shown below, where the cross section is reduced due to the presence of gas hydrates, the ellipse fitting does the best job it can (error minimization), as shown by the purple oval. The centre of the pipe cannot be determined anyway, as the fingers are not touching the pipe wall. So in situations like this the interpreter must understand that the measurements after centralization can be displaced, and therefore care should be exercised when reporting the statistics (max/min ID, penetration, reduction, etc.)

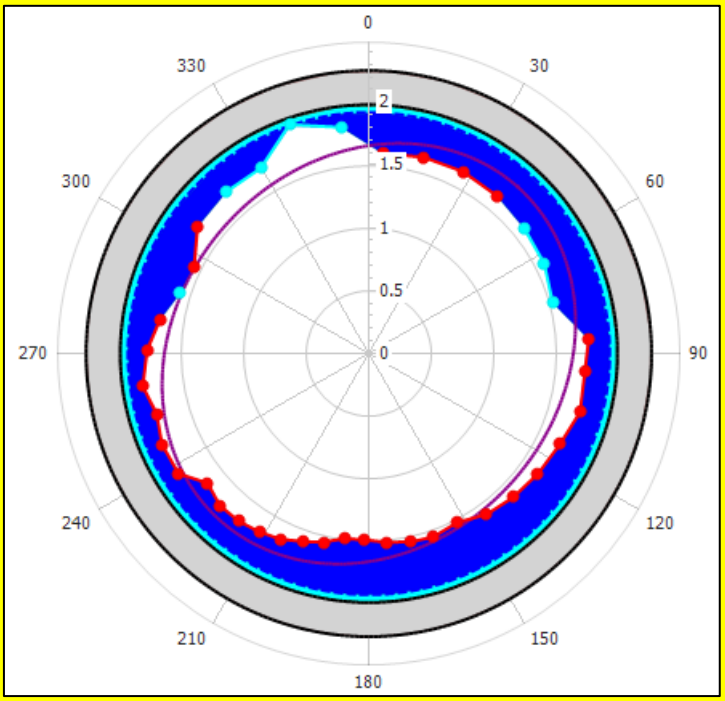

Fig. 18 – Centralization in presence of gas hydrates

A special case, however, is when the pipe is actually deformed, like a lateral displacement. In this case, it is not advisable to apply the centralization blindly. This will be explained later.

3.2. Re-Calibration

For MFC processing, the word 'Calibration' was previously used for the operation of transforming the finger's electrical response to a radius value. This is achieved by a number of surface calibrations, both isothermal and using a number of temperature steps.

'Re-calibration' is applied if the computed radius values using the surface calibrations, are no longer representative of the internal pipe radius. This can occur due to a number of reasons:

- Finger tip wear: The dimensions of the fingers may have changed compared to the surface calibration, as the finger tip scratches the inner surface of the pipe.
- The electrical properties of the circuit (especially the inductance) may not be the same as it was originally. This can cause some drift on the measurements.
- Not valid calibration: The calibration file may not correspond to the specific survey, may be out of range, etc.

If one of these situations is present in certain (full log or partial) dataset, there will be a consistent positive or negative difference between the finger reading and the actual radius it should measure.

If all fingers show an error in the same direction and magnitude (i.e. positive offset of 0.05 in) then it may be challenging to differentiate it with respect to an actual metal loss or deposition. Fortunately, in most cases the need for re-calibration can be assessed by looking at the MFC image, MFC radius and by extracting the radius measurements at different depths:

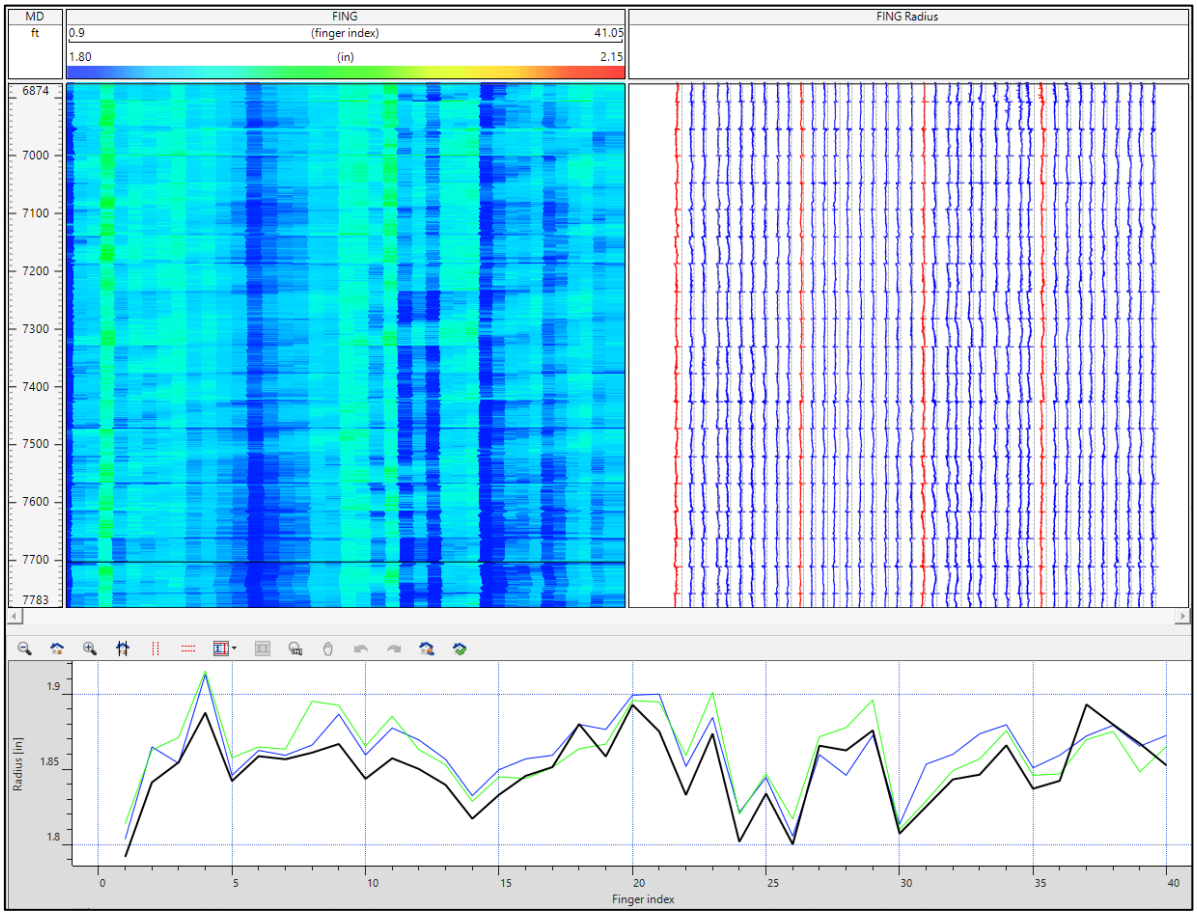

Fig. 19 – Assessing the need of re-calibration

- The MFC image uncorrected for bearing shows a striped behavior, which is typically present in multiple joints.
- The MFC radius shows that the offset between the nominal ID (dashed lines) and the measurement itself varies significantly for the different arms.
- The radius measurements at different depths show a repeatable behavior, with some arms always measuring higher or lower than the mean.

Once the MFC data is loaded into Emeraude, it is no longer an option to apply a re-calibration in the same fashion as the original calibration. This is because the actual pipe radius is not known and it varies with depth, with the different penetration and deposition features. An alternative approach is used, which consists on calculating the average radius value for all the fingers over a certain recalibration interval. These averages are then compared against:

- Mean or median of all the fingers over the same interval
- Known ID (nominal) over the same interval.

The difference between the average finger radius (RADi) and the overall MFC radius as obtained by one of these two methods is used to compute the individual fingers shifts. These shifts will be different for each arm, and will be applied at every depth of the selected interval:

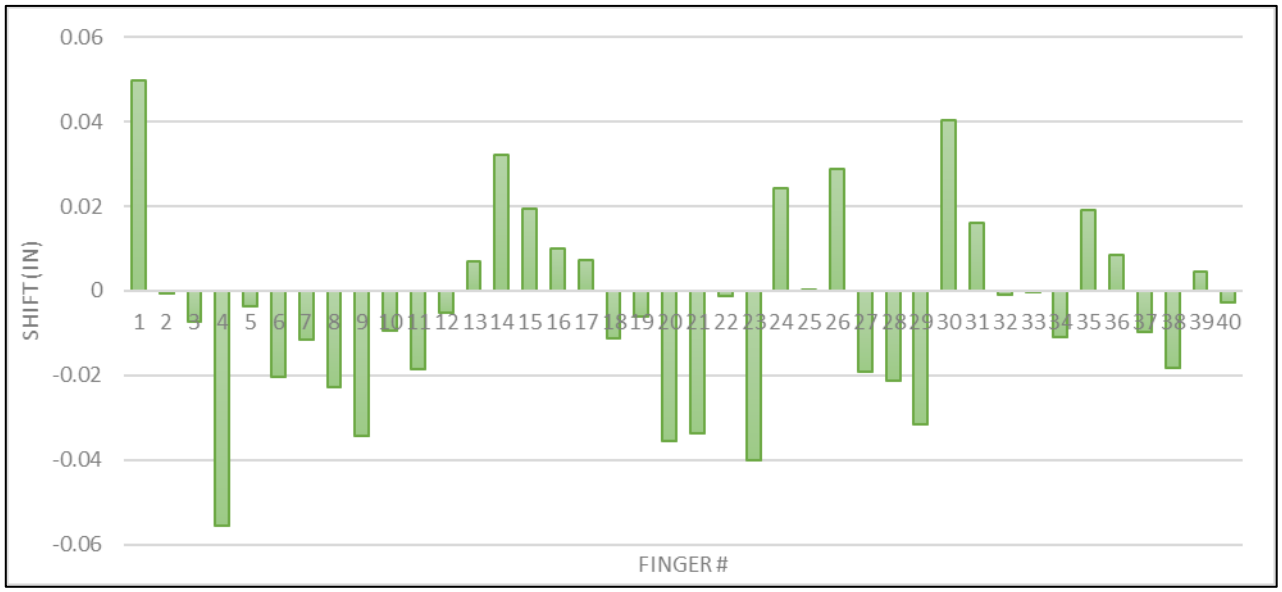

Fig. 20 – Calculated shift per finger

For using the first approach, where a statistical value (median or mean) is applied, it is necessary to ensure that the recalibration interval includes only pipes of the same size (OD, weight). It is also important that the selected interval does not include areas of severe damage or deposition, which can lead to non-representative statistics.

The second approach, which uses a known ID, should only be applied when there is good confidence that the tubulars have the same ID than the informed nominal. When the pipe has suffered metal loss or deposition, this is no longer true. However, even for new pipes in good

condition, there is a 12.5% thickness tolerance. Valves, nipples and other special completion elements have stricter dimensional tolerances, and therefore these are preferred for using the 'known ID' recalibration method.

A single recalibration zone may be enough, if the surveyed pipe size is constant and there is no evidence of drift. Otherwise, different recalibration zones are needed, in order to apply zonal shifts.

The image below shows the same depth range as Figure 19, but in this case the interval marked in red has been re-calibrated The radius are much more homogeneous, there is evidence of spiraling (manufacturing-induced small ovalization), and the extracted arms in black (inside re-calibrated interval) show much lower variance than the green and red curves (outside the interval). Clearly the lack of re-calibration was shielding the real pipe features. In this case it would be necessary to recalibrate the whole depth range.

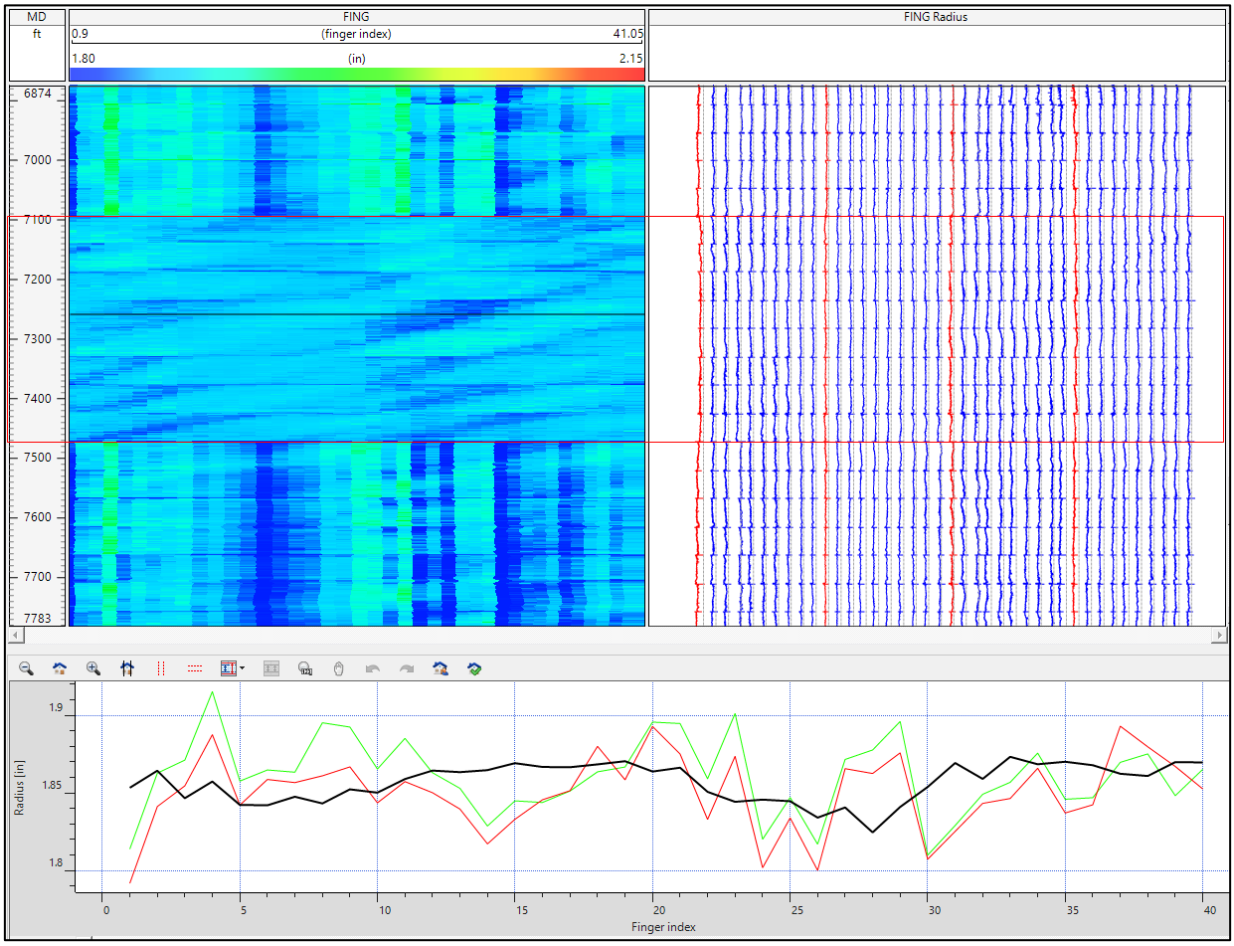

Fig. 21 – Calculated shift per finger

FAQ 4: Re-calibration after Centralization. Is the data ready?

Clearly, it is necessary to perform a centralization before re-calibrating the fingers. In case the user does not explicitly run the centralization before, when the re-calibration is launched, a default centralization will be automatically applied by Emeraude (not persisted).

So the question is, after centralization and recalibration, is the data ready for obtaining the statistics per tubing or casing joint?

The original centralization included data that was later modified, by the applied recalibration shifts. Therefore, the original data may have contained outliers that were excluded from the centralization, but these were not real pipe characteristics but artefacts due to improper fingers calibration.

By looking at the pre-recalibration data on Figure 19, it can be clearly seen that Fingers 1, 24, 26 and 30 consistently measure lower values, which is confirmed by the shift magnitudes displayed in Figure 20. When the centralization is applied to this data, the excluded arms are exactly those mentioned before:

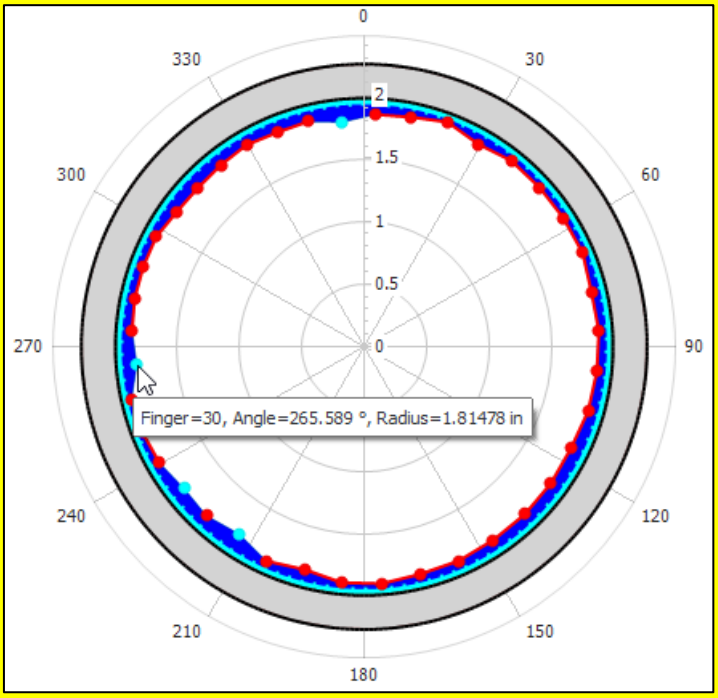

Fig. 22 – Original (pre-recalibration) centralization

Obviously when the recalibration shifts are applied, the shape of the data will change. The fingers that were originally taken as outliers will not necessary be off from the centralization shape after recalibration.

In conclusion, if a recalibration was applied after the centralization, a new (second) centralization may be necessary, especially when the magnitude of the shifts was significant.

3.3. Joints Identification

Different types of threaded connections can be found in the surveyed tubulars. 'Integral connections' refer to cases were two joints are connected without using an intermediate tubular. These can be 'upset' or 'Non-upset' (flush), whether the pipe end has an increased wall thickness or not. On the other hand, coupled connections connect two casing joints through an externally threaded short tubular.

Regardless of the connection type, when reporting the diameters and statistics of the surveyed pipe, we want to remove the influence of the connections. The figure below shows two different connection types. If the statistics were to include the connections, the one on the left would show as an increased penetration, while the one on the right would be a peak on the reduction:

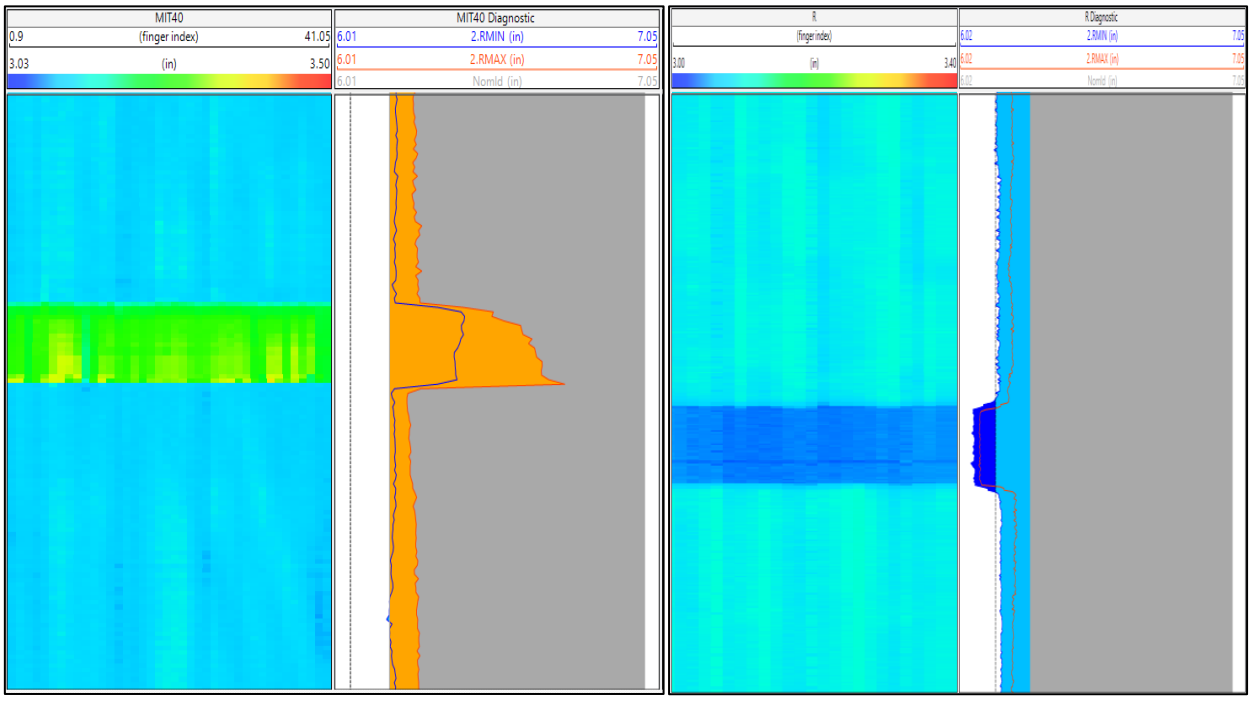

Fig. 23 – Different connection types

In the above-shown cases, the connections can be easily identified through the penetration or metal loss tracks. Alternatively, a CCL can be used as primary source of the connection location. In Emeraude this is done by setting, manually or interactively, a threshold value on one of these tracks.

The identified tubing or casing joint should remove, apart from the connection itself, the surrounding pipe which is affected by the connection itself. As seen below for an upset connection, the internal diameter is smaller above and below the connection. This part is not representative of the main pipe body. In Emeraude, an offset between the position where the threshold intersects the reference curve and the beginning of the joint can be established:

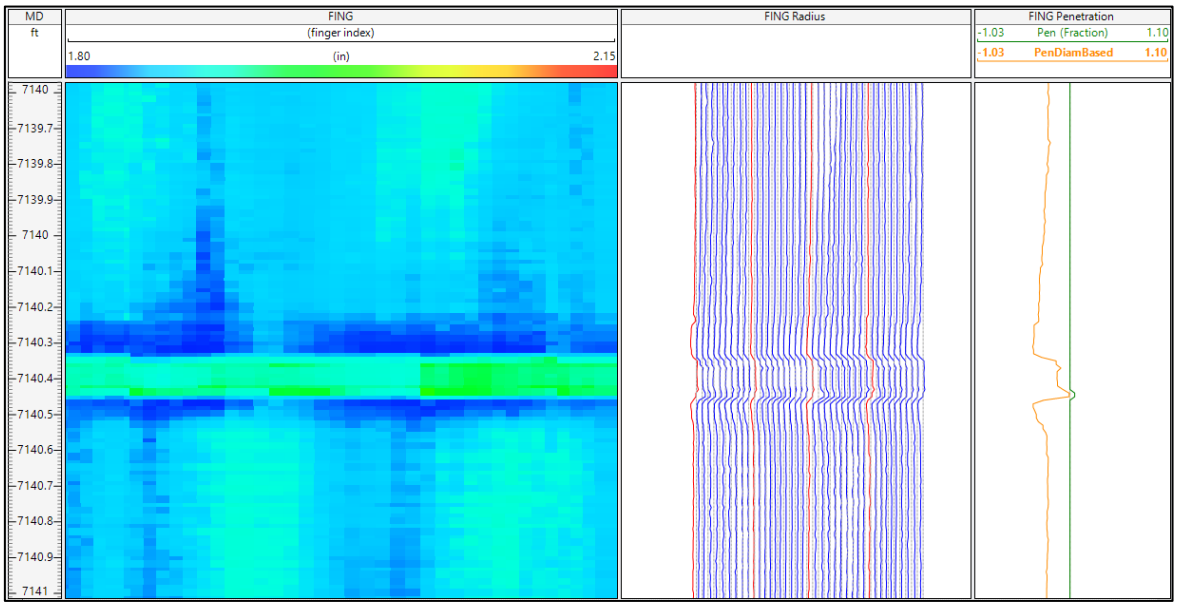

Fig. 24 – Affected pipe around the connection

4. MFC Results

After the MFC data has been processed, a number of statistics will be computed for every depth of the log. These will be presented vs. depth as logs and tabulated for every identified joint.

As the MFC measures radii values for each finger, the primary statistics at any depth will be the Maximum and Minimum Radius (RADMAX and RADMIN), the radius average (RADAVG), the median (RADMED) and the standard deviation of the radii measurements.

It is also convenient to express the results as diameters. The opposite finger's radii are summed up to compute *n/2* diameters (where *n* is the number of fingers). The same statistics as explained above for the radii values are computed. We will see below that the maximum and minimum ID calculated as the sum of opposite arms (IDMAX and IDMIN) may not be appropriate to represent the actual condition of the pipe:

Penetration and maximum ID

At every depth, the maximum radius is established. The penetration represents the pipe's internal metal loss relative to the pipe thickness, as:

$$Penetration = (2 * RADMAX - IDNOM)/(ODNOM - IDNOM)$$

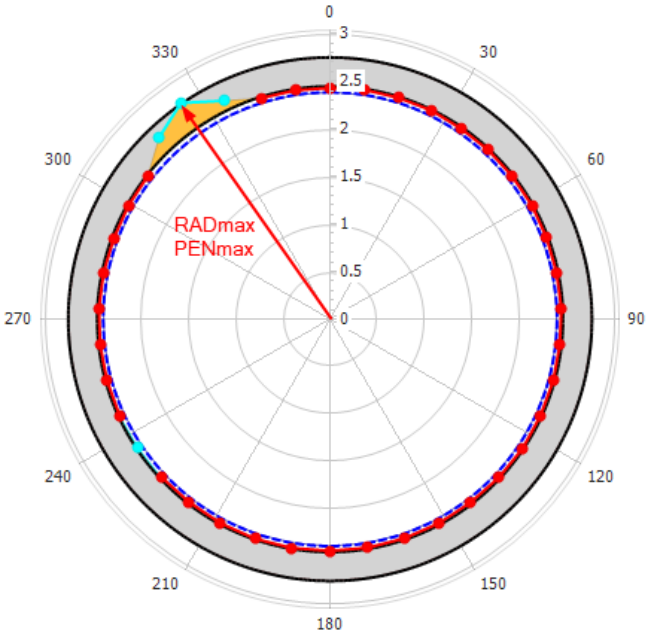

*Fig. 25 – Maximum ID (2*RADMAX) and Penetration*

FAQ 5: Double radius or sum of opposite arms?

The penetration equation works with diameter values (IDNOM, ODNOM), but instead of showing directly IDMAX it says '2*RADMAX'. Why is that?

Let's imagine that in this case the arm showing maximum penetration (at around 325 deg) is exactly a fully penetrating feature (RAD= OD/2). The opposite arm (145 deg), does not sense any penetration (RAD= ID/2). If we were using opposite fingers diameters, the penetration value would be 0.5 (50%). This is indeed counter-intuitive, since we actually have a full wall penetration.

Therefore, for IDMAX and IDMIN we use 2*RADMAX and 2*RADMIN in the MFC Diagnostic track, in the Joints table and to calculate the penetration and reduction.

Metal Loss

Similar to the Penetration, the metal loss is a representation of how much the radius goes above nominal ID. However, the metal loss considers all the fingers (compared to the one of RADMAX in the penetration), giving a cross-sectional average indication of the wall thickness reduction.

$$MLOSS = \frac{1}{n * ID} \sum_{i=1}^{n} (RAD_i - \frac{ID}{2})$$

As seen in the image below, the metal loss reduces the influence of localized pitting by averaging all the fingers. It may also be misleading when there are 'as manufactured' joint variation, as observed between joints 58 to 60.

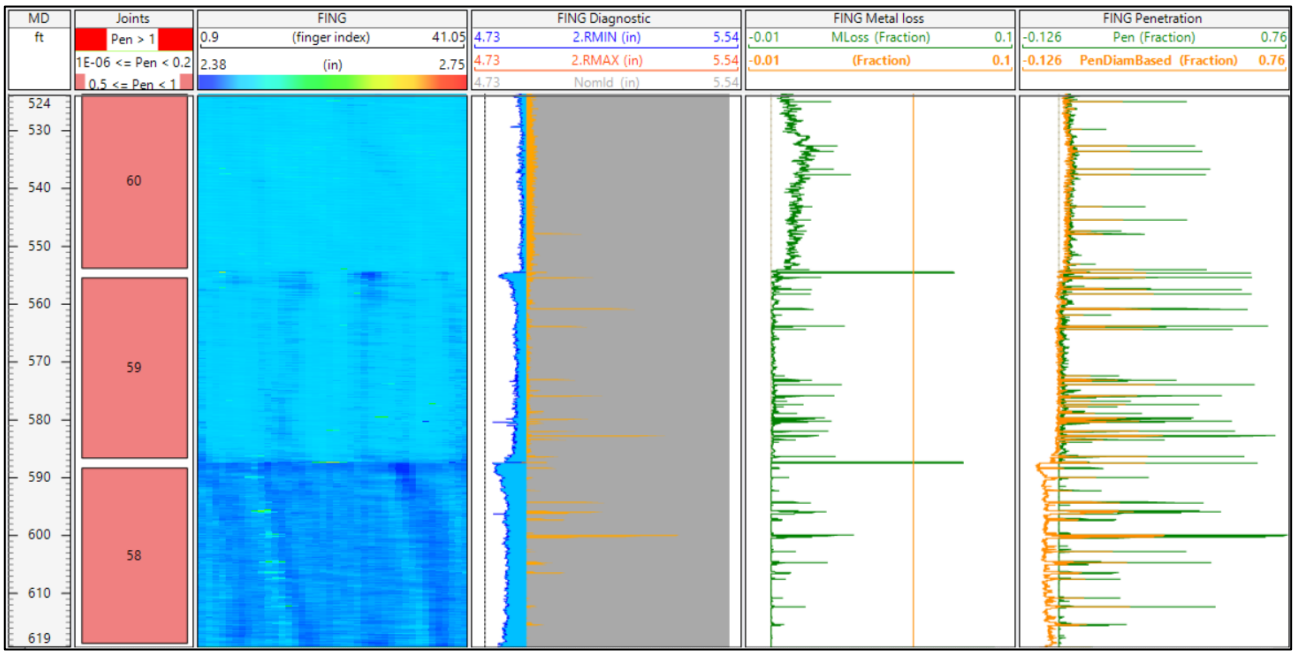

Fig. 26 – Metal Loss and Penetration

This statistic is sometimes used to determine the remnant mechanical properties of the pipes, since these properties are a stronger function of the generalized metal loss than isolated pitting (that would be represented by the Penetration statistic).

Reduction and minimum ID

At any depth, the minimum ID is established based on 2*RADMIN (for the reasons explained above).

The minimum radius is used to calculate the reduction value as:

$$Reduction = \frac{\frac{ID}{2} - MINRAD}{\frac{ID}{2}}$$

A reduction of one (not possible as the minimum radius is limited to the closed MFC value) means that a circular object going through this can only occupy half of the pipe.

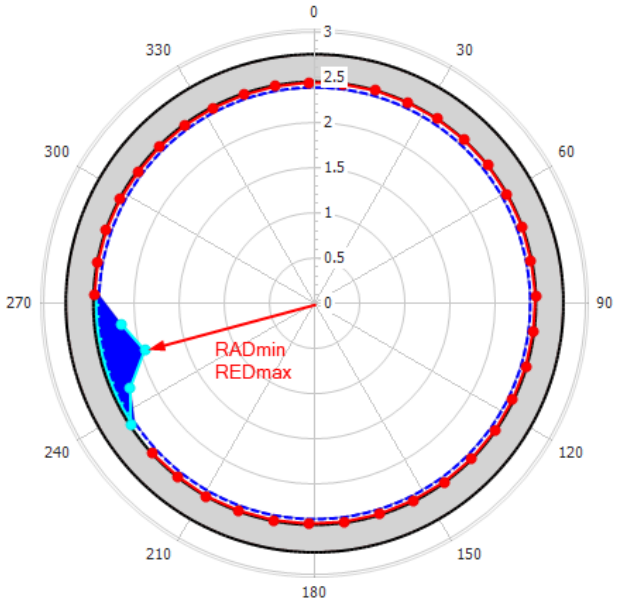

Fig. 27 – Minimum ID and Reduction

Ovalization

Pipe ovality refers to the distortion of the cross-section of the tubular from its normal, circular shape. This is a key statistic for plug or packer setting, since the larger is the ovality, the worse will be the sealing. Different practices establish a maximum acceptable ovality to consider that certain depth is adequate as a plug setting depth.

The ovalization is calculated as:

$$Oval = \frac{(IDMAX - IDMIN)}{IDAVG}$$

In this case, the opposite fingers IDMAX and IDMIN are used. If these values were equal, ovality would be zero.

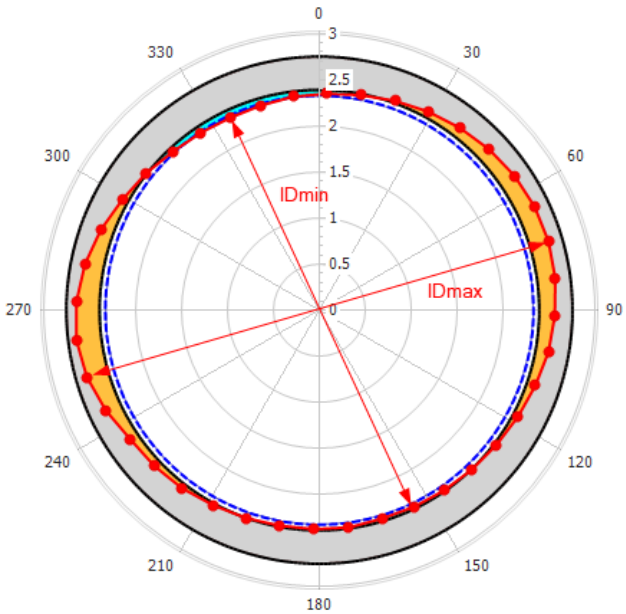

Fig. 28 – Ovalization

Note that there are different definitions of pipe ovality from the different available standards and recommended practices. Make sure you know which equations they use.

FAQ 6: What is the nominal pipe ID?

Most of the casing and tubing are manufactured according to API 5CT (ISO 11960) standard. Due to the manufacturing process, it is difficult to measure the internal pipe diameter with high accuracy. Therefore, this standard establishes tolerances on the outer pipe diameter (easier to measure than the ID), as follows:

- For pipe less than 4.5'', the tolerance is +/- 0.79 mm (+/- 0.031 in)
- For pipes equal or larger than 4.5'', the tolerance is + 1% to -0.5% OD

The internal diameter is then estimated based on the pipe weight and material density, which will allow us to calculate the pipe thickness and therefore the ID. The pipe mass, in turn, also has an associated tolerance (i.e. 6.5% to -3.5% for single lengths).

For these reasons, API 5CT establishes the well know 12.5% permissible under tolerance on the pipe thickness. This is sometimes known as the 'API penetration tolerance'.

This uncertainty will impact on the accuracy of different calculation, such as the penetration, metal loss, and as will be explained later, on the mechanical properties of the pipe.

Stringent well design planning typically includes a baseline MFC, run while or straight after the well completion. This would provide a valid 'nominal' ID of the pipe, that can be used in time-lapse MFC to accurately estimate the evolution of the pipe thickness variations.

In general, the default option remains the nominal ID as established in the pipe catalogue. When there is strong evidence of 'as manufactured' smaller pipe thickness, some interpreters already account for the 12.5% of thickness reduction. Other option would be to use a statistical value, for example, when localized pitting is present, then is possible to use the average or median joint ID as the nominal ID.

Make sure you understand how the error on the nominal ID propagates into the different results and choose the right approach.

Status of completion elements

The statistics presented in this section are, in general, used to describe the condition of the tubing, casing and pup joints. As shown in Figure 17, when completion elements are surveyed, they show abnormal penetration or reduction values, so these are typically excluded from the final summary table. However, just by visual inspection it is possible to extract important information.

For example, Sliding Sleeves (SSDs) can be shifted open or closed through wireline or coiled tubing intervention, to above unwanted fluids or improve the reservoir sweep. In order to verify the current position of the SSD, it is possible to compare the MFC signature with the open and close fingerprints. The image below shows the same sliding sleeve in open and closed positions.

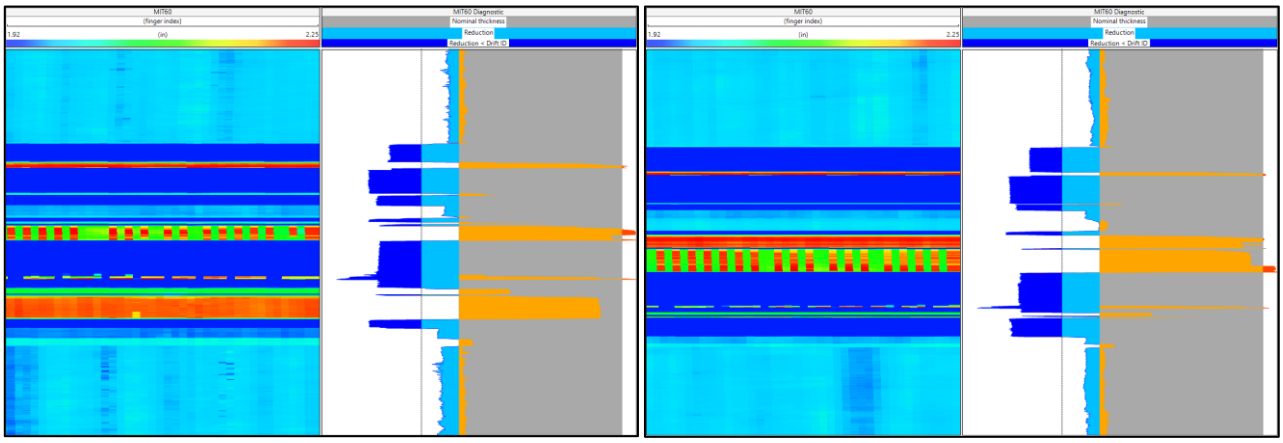

Fig. 29 – SSD status. Left: Open – Right: Closed

It is useful to keep snapshots of the MFC image and diagnostic of different completion elements. This helps to quickly diagnose the status of these elements, look for problems (partially open/closed, deposition, deformed, etc.). The fingerprints can be recorded both in-situ (downhole measurements) or through yard logging. The latter allows for better control of the operation and the condition of the element (inverted, full/partially open, etc.).

5. Mechanical properties calculation

This section is an introduction to the calculation of the remnant pipe mechanical properties based on Multitier Caliper results. This analysis will help us to understand if the surveyed pipe is still fit for service and/or if it would withstand a well operation, which typically includes pressurizing the pipe or annulus (killing the well, cementing, fracking, venting, etc.).

By no means this is an exhaustive treatment, and the equations presented below should be applied with extreme care, given the number of assumptions used to derive them. The American Petroleum Institute Standard API TR 5C3 (*Calculating Performance Properties of Pipe Used as Casing or Tubing*) details the equations and their hypothesis. This section will briefly show how the MFC-calculated pipe dimensions of the surveyed pipe can be used to update the mechanical properties.

5.1. Theory background

In Mechanics of materials, structures as pipes are treated as 'Thin-walled pressure vessels'. The second part of this definition refers to the fact that these structures are capable of holding internal pressure. The concept of thin wall implies that, as the ratio of t/d is so small, the distribution of the normal stresses on a cut is essentially uniform through the thickness of the shell. This also allow us to conclude that the stress condition on the outer surface is planar, comprised by a longitudinal stress (σ_z) and a tangential or 'hoop' stress (σ_θ).

If we consider a pipe subject only to internal pressure, a free body can be used to obtain the magnitude of the hoop stresses.

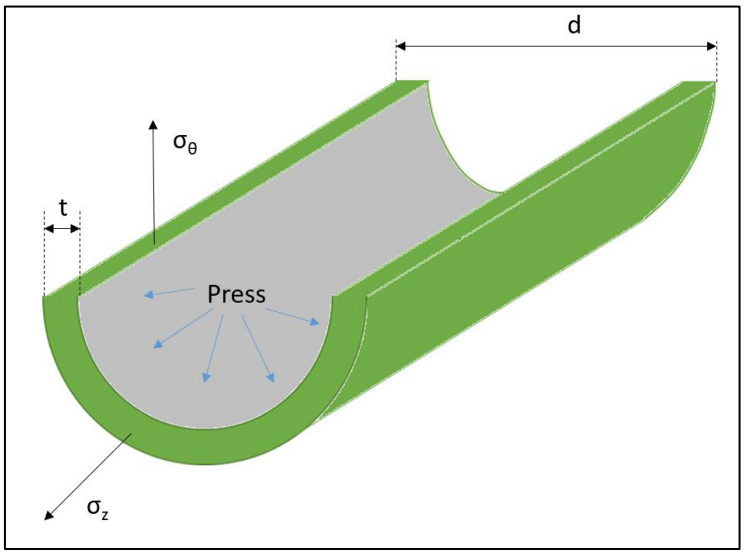

Fig. 30 – Stresses on a pipe subject to internal pressure

The resulting stresses can be calculated using the following equations:

$$\sigma_\theta = \frac{Pd}{2\,t}$$

This equation is commonly known as Barlow's Formula. If the tension reaches a critical value, 'burst' will occur.

If a pipe is subject to an axial load *F* (i.e. hanged tubing withstanding its own weight or compressional force while running the casing) the experienced longitudinal stress will be equal to:

$$\sigma_z = \frac{4\,F}{\pi\,(OD^2 - ID^2)}$$

Therefore, through this formula it is possible to calculate the maximum load for tensile failure, when the stress reaches for example the yield stress (more on this below). This formula can also be applied for compressive axial loads; however, pipes may undergo compressive axial buckling before reaching compressive failure.

Finally, a pipe subject to a high external pressure can undergo 'collapse'. We will see later that API presents different equations for collapse pressure, depending on the thickness to OD ratio. At this point it is important to mention that some of these equations can be derived analytically from the Lamé equation for thick wall pressure vessels. Compared to the Barlow's formula, in thick wall pipes the hoop stress varies along the shell (maximum on the inside) and there is a net radial stress component. The hoop stress obtained from the Lamé equation at the internal radius can be expressed as:

$$\sigma_\theta = \left[\frac{d_o^2 + d_i^2}{d_o^2 - d_i^2}\right] P_i - \left[\frac{2\,d_o^2}{d_o^2 - d_i^2}\right] P_o$$

These equations were derived for perfectly circular pipes. However, experimental data and finite element simulations show that the collapse pressure decreases significantly with pipe ovality.

At this stage we have formulated the concepts and equations of four typical tensional stresses that can be found in pipes: Burst, Collapse, Compression and Tension. The theory presented above is the base of API TR 5C3, and the collapse failure criteria under one of these states will be evaluated as a uniaxial stress state. In general, pipes will be subject to other loads, including buckling, torsion, etc., which are beyond the scope of this material. Bi-axial and Tri-axial stress models are commonly used by well design engineers, where the different stress components are combined using the Distortion Energy Theory, known as Von Misses equation.

Again, we will focus on the API definitions, where failure occurs when one of the uniaxial stress states reaches a critical stress of the material, called Yield Strength.

FAQ 7: What is the strength of the pipe?

API 5CT specifies the technical delivery conditions for steel pipes. The steel grades are designed by a code like K55, L80, P110, etc. The prefix letter designation has no special meaning. The number following the letter corresponds to the Specified Minimum Yield Strength (SMYS) of the pipe in Ksi (thousands of psi). For example, the steel grade L80 has a SMYS of 80000 psi.

As an industry practice, it is established that casing and tubing strings are limited to the elastic stress-strain regime. Therefore, the API Standard considers the Yield Strength as the critical stress for failure (typically with a safety coefficient).

The actual material strength (Ultimate tensile strength – UTC) is greater than the Yield strength. However, for design purposes the elastic regime is considered, which means that if the material is unloaded, the strain will go back to zero (original length).

5.2. API Definitions

The API TR 5C3 Standard presents the formulas that will be used to calculate the remnant mechanical properties of the pipe. We will focus on the Burst and Collapse pressures using the uniaxial approach, as opposed to the complete triaxial calculation. Calculating other stress components require more inputs from the cement, completion string, temperature effects, etc., that won't be accounted for in this analysis.

It cannot be stressed enough that these formulas have to be treated with caution. Catastrophic failures due to burst or collapse may involve human lives, environmental consequences and (of course) lawyers.

It is also important to understand that the API standard does not mention at any point the words Multifinger Caliper or Magnetic/ultrasonic thickness. This means that there are no indications to new or used pipes. In the next section we will discuss some considerations of applying these equations to MFC data.

Burst Pressure

Based on Barrow's formula, using the yield strength as maximum allowed. As there is a 12.5% tolerance on the pipe thickness (API 5CT), a factor 0.875 accounts for the minimum wall thickness:

$$P = 0.875\,(\frac{2\,Y_p\,t}{D})$$

Collapse Pressure

The collapse pressure calculation includes four regions, depending of the t/D ratio. The regions are called: Yield collapse, Plastic collapse, Transition collapse and Elastic collapse. The formulas for the Yield and Elastic collapse can be theoretically derived (Lamé). The formula of Plastic collapse is empirical, while the Transition formula accounts for the cases between elastic and plastic collapse pressures.

- Yield Collapse: The necessary external pressure for the hoop stresses (Lamé) to reach the Yield stress (so not necessarily a true collapse):

$$P_{Y_P} = 2\,Y_P \left[\frac{\left({}^{D}/_{t}\right) - 1}{\left({}^{D}/_{t}\right)^2}\right]$$

  This formula is applicable to D/t values up to the intersection with the plastic collapse formula, given by:

$$(D/t)_{YP} = \frac{\sqrt{(A-2)^2 + 8\,(B + \frac{C}{Y_P})} + (A-2)}{2\,(B + \frac{C}{Y_P})}$$

- Plastic collapse: Experimentally-derived equation which predicts the necessary external pressure to cause plastic collapse (permanent deformation):

$$P_P = Y_P \left[\frac{A}{D/t} - B\right] - C$$

  This equation is applicable for D/t from $(D/t)_{YP}$ to the transition with D/t transition:

$$(D/t)_{PT} = \frac{Y_P\,(A-F)}{C + Y_P(B-G)}$$

- Transition collapse: In the transition zone between plastic and elastic, the necessary pressure to cause collapse can be calculated as:

$$P_T = Y_P \left[\frac{F}{D/t} - G\right]$$

  This equation is applicable for D/t from $(D/t)_{PT}$ to the transition with D/t transition:

$$(D/t)_{TE} = \frac{2 + B/A}{3B/A}$$

- Elastic collapse: In this region it is predicted that the pipe will lose its elastic stability under the action of an external pressure. Note that the formula below, which is theoretically derived, is not a function of the pipe yield strength, as this collapse type is dependent on the elastic modulus and geometry only.

$$P_E = \frac{46.95\,10^6}{\left(\frac{D}{t}\right)(D/t-1)^2}$$

  Applicable for D/t >= $(D/t)_{TE}$

The constants for different API pipes are presented in the table below:

Steel Grade	D/t Range			Plastic Collapse Pressure Factors			Elastoplastic Collapse Pressure Factors	
	$(D/t)_{YP}$	$(D/t)_{PE}$	$(D/t)_{TE}$	A	B	C	F	G
H40	16.4	27.01	42.64	2.95	0.0465	754	2.063	0.0325
J/K55	14.81	25.01	37.21	2.991	0.0541	1206	1.989	0.036
J/K60	14.44	24.42	35.73	3.005	0.0566	1356	1.983	0.0373
L/N80	13.38	22.47	31.02	3.071	0.0667	1955	1.998	0.0434
C90	13.01	21.69	29.18	3.106	0.0718	2254	2.017	0.0466
C/T95	12.85	21.33	28.36	3.124	0.0743	2404	2.029	0.0482
P110	12.44	20.41	26.22	3.181	0.0819	2852	2.066	0.0532
Q125	12.11	19.63	24.46	3.239	0.0895	3301	2.106	0.0582
A140	11.84	18.97	22.98	3.297	0.0971	3751	2.146	0.0632
A150	11.67	18.57	22.11	3.336	0.1021	4053	2.174	0.0666

5.3. Remnant mechanical properties

A well that was designed to withstand the certain level of pressures and mechanical loads many years ago when the casing and tubing joints were new, may not necessary support these currently or in the future, when corrosion or erosion have taken its toll. This becomes critical when planning workovers, side-tracks, P&A, refracking, etc.

The formulas presented in the previous section are all a function of the pipe thickness. Even before running the completion there is an unknown on this (API tolerance), which requires the use of safety factors. Once the completion is in place, the only way to obtain the wall thickness is by running downhole measurements.

Pipe thickness can be calculated as $t = \frac{(OD-ID)}{2}$

When using MFC as the primary source of pipe thickness, we must take into account a number of points:

Outer pipe diameter

Corrosion on the outer may decrease the pipe thickness, and the MFC tool will not account for this. In the absence of a pipe thickness measurement (i.e. magnetic), the engineer should make a big assumption on the outer pipe diameter. Setting the OD equal to the nominal pipe OD may not always be safe for cases where the external pipe wall is in contact with the different reservoir fluids (i.e. non cemented intervals), tubing with liquid-filled annular, etc.

As mentioned in FAQ 6, API 5CT establishes a tolerance on the external pipe diameter, which will definitely have an impact on the thickness calculation, especially for small thickness pipes.

Initial Internal diameter

The issue of using nominal internal diameter as reference value to calculate the metal loss and reduction statistics becomes evident when analyzing the implications on the mechanical properties calculation. The dimensional tolerance specified by API, allows certain room for ID variation change. 'As manufactured' joint variations are shown in the image below. Some of the joints fall below nominal ID, but still remain above drift ID. When comparing to the joints above and below, it is clear that this in not deposition, as it wouldn't occur only in those two pipes and in such a homogeneous fashion. These pipes show cero metal loss, but this was calculated using nominal ID as reference.

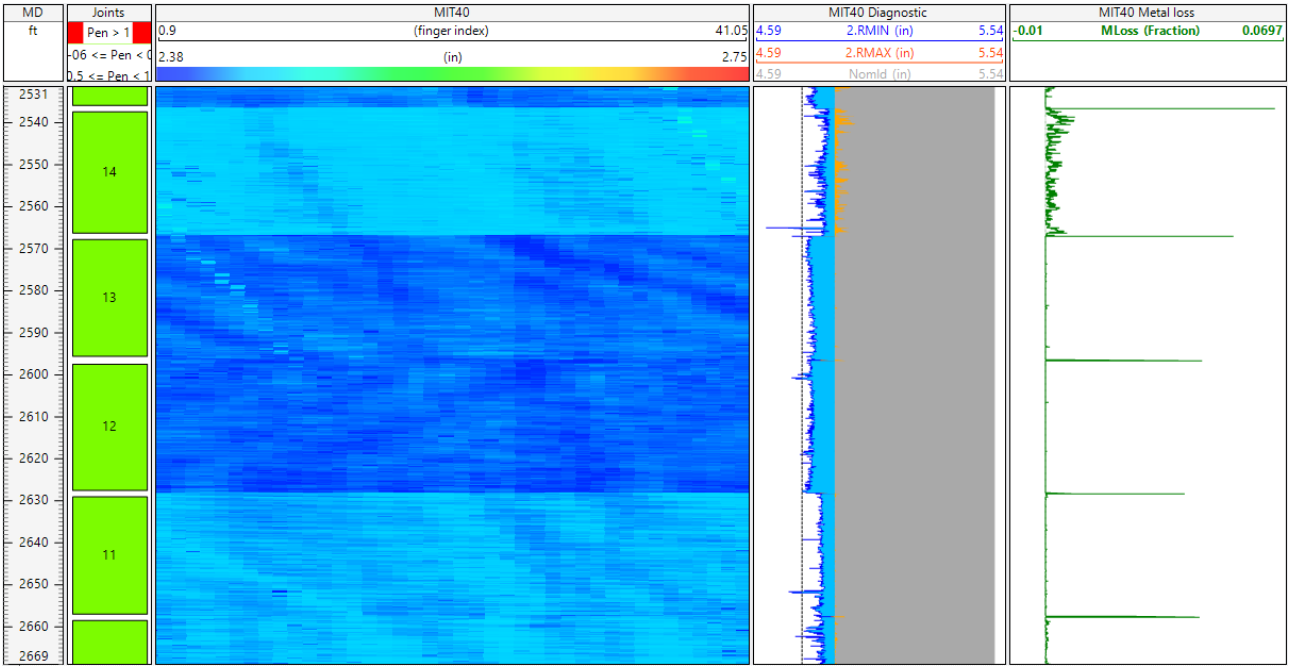

Fig. 31 – As manufactured joint variations

This image also shows the benefits of running a baseline MFC, straight after running the completion or early in the life of the well.

Current Internal diameter

Once we run the MFC, we will end up with a number of diameter computations, like ID average, ID mean, ID max, ID min. So the question is, what diameter should I use to compute the pipe thickness? Again, there is no reference to this on the API standard.

Let's consider two possible cases:

- **Isolated pitting**: A number of isolated, not-fully penetrating pits are showed in the image below, reaching penetration values up to 70%. Using the maximum ID to calculate the pipe thickness would imply a reduction of the burst pressure of 70% compared to the pipe with nominal ID. However, it can be seen that the mean ID did not varied significantly with respect to the nominal ID, giving a low overall metal loss (average 1%).

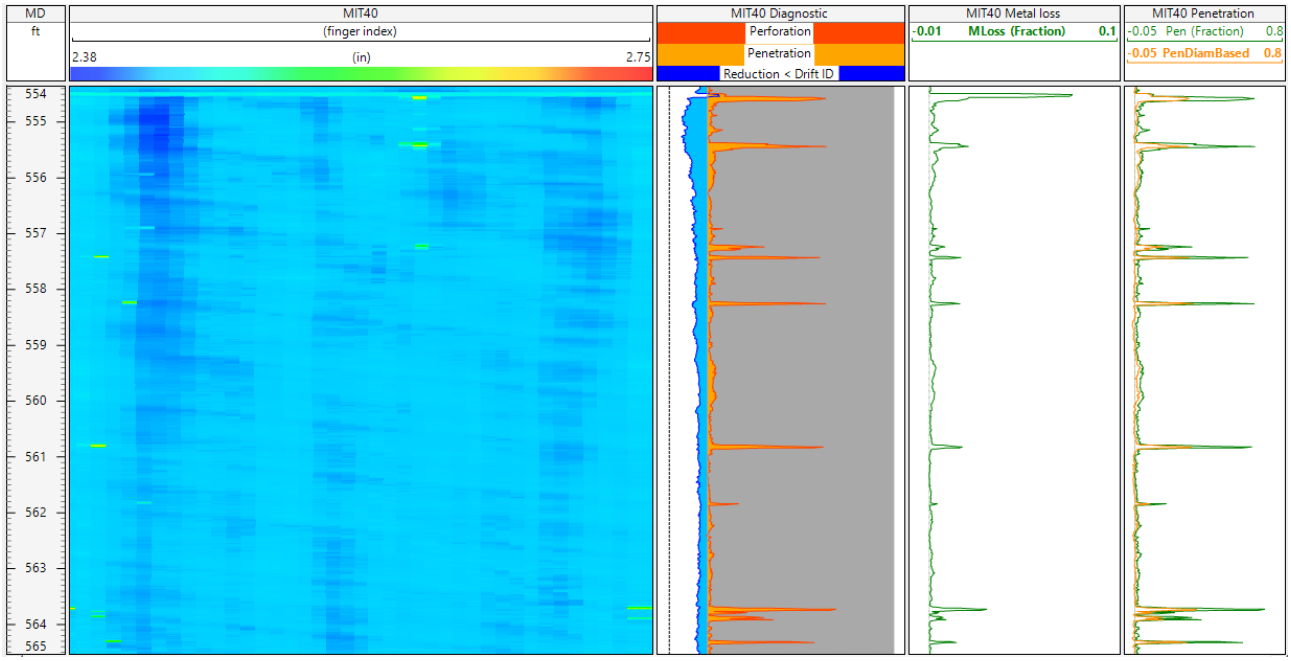

Fig. 32 – Isolated pitting

This is an interdisciplinary decision that should be taken understanding the mechanism of corrosion and their morphology. In this case, high CO2 concentrations allow us to anticipate sweet corrosion, where indeed the morphology is isolated pitting. Actually, the field experience suggests that the failure mechanism from CO2 corrosion in tubing is leakage in the annulus, rather than an overall loss on the mechanical properties that may lead to early burst.

Recommended practices (i.e. DNV-RP-F101 'Corroded pipelines') introduce the definition of Single Defect and Interacting Defect. In single defects, the failure pressure is independent from other defects. However, when there is interaction, the failure pressure will be lower. Whether the defect is isolated or not is based on the circumferential and or axial spacing between adjacent defects:

$$\emptyset > 360\sqrt{\frac{t}{D}}$$

$$s > 2\sqrt{Dt}$$

So in this case, the presence of the isolated pitting does not affect the overall pressure-bearing capacity of the pipe, and the mean ID can be used to estimate the current diameters.

- **Homogeneous metal loss:** When uniform corrosion is present, the Metal loss will be closer to the penetration value. The image below shows such a case, where it can be seen that there is a circumferential metal loss, and this indeed would have an effect on the remnant mechanical properties of the pipe.

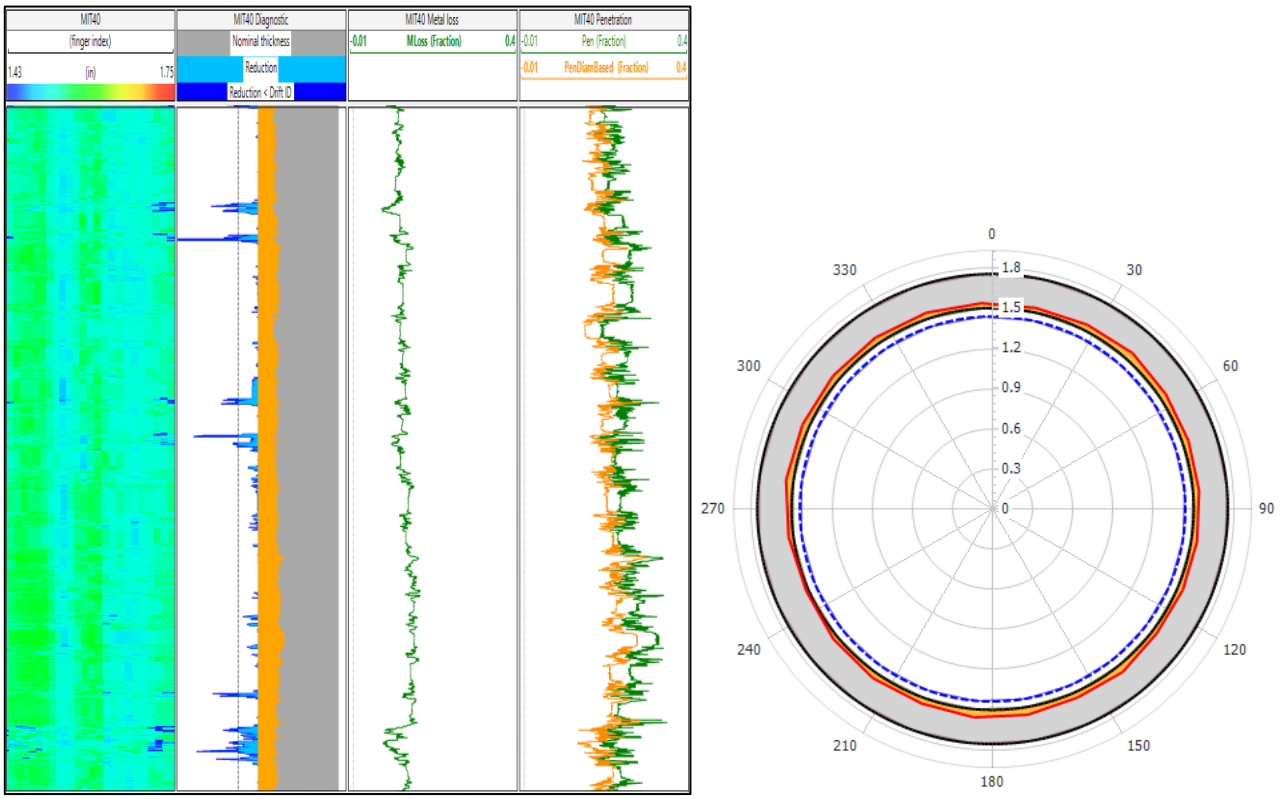

Fig. 33 – Uniform corrosion

These two examples demonstrate the different choices of internal diameter that may need to be used, and are by no means recommendations on future decisions on the calculation of mechanical properties.

Some companies directly talk in terms of maximum allowable metal loss or pipe wear. Assuming homogenous corrosion, the API Burst pressure prediction is inversely proportional to the metal loss, as shown in the image below:

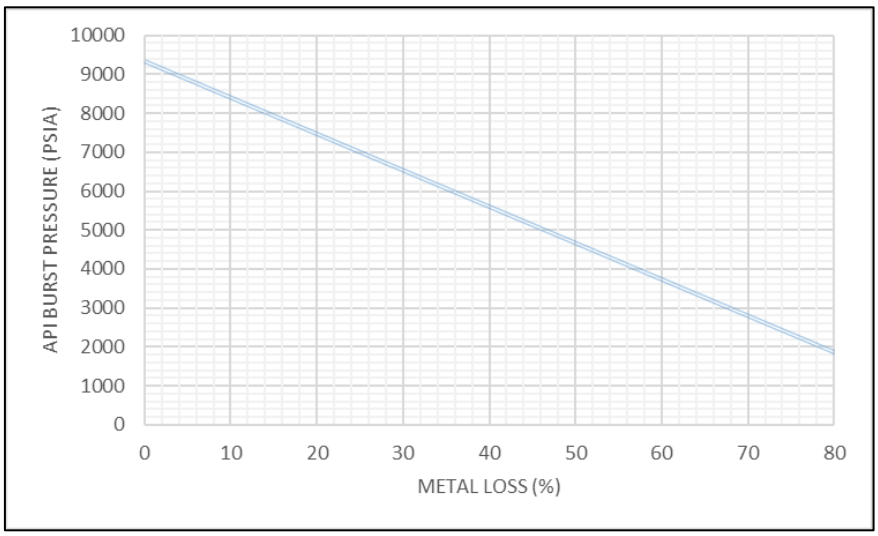

Fig. 34 – Burst Pressure as a function of Metal loss for a 7 in (29 lb/ft) L80 casing.

6. Pipe deformation

At this stage of the document, the reader should have a fairly good idea on how to obtain a number of pipe statics from a raw MFC dataset, and how these can impact on the mechanical properties of the pipe.

We will consider now the case where the stresses in the formation or the loads during the well completion deform the pipe. With 'deformed pipe' we refer to a loss on the circularity (i.e. ovalization) or a modification of the original pipe trajectory (lateral displacement). These cases would not raise any flag in the statistical results covered in the previous section, so it is important for the user to understand what images and curves may help to diagnose deformation.

Severe cases of pipe deformation are typically related to well access problems. Ovalization can cause issues like packers or plugs which do not seal, leaks on casing hangers, and eventually it may not be possible to intervene the well, passing through this region. For lateral displacement cases, it can also happen that due to the tortuosity of the pipe the well cannot be re-entered, creating numerous problems for the design of any remedial workover, stimulation, and ultimately P&A.

6.1. Stresses in the earth's crust

If we consider a small cube of formation, buried somewhere in the earth crust, we will found that it is subject to a complex stress condition, which can be represented by the stress tensor. In general, this is a 9 components tensor, but due to equilibrium symmetry, the shear stresses S_{ij} will be equal to S_{ji}. Still, this gives us a 6 independent components stress tensor, which would be quite complex to characterize. Fortunately, we know that it is possible to apply a tensor transformation, in order to orient this cube in such a way that the only components of the stress tensor are the principal components, as shown in the image below:

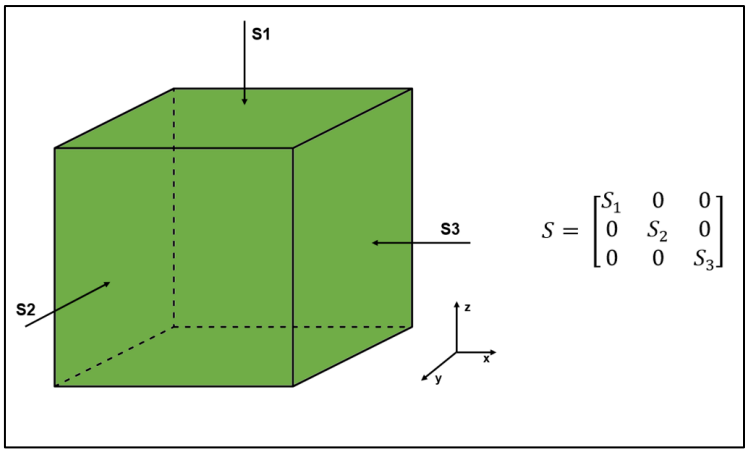

Fig. 35 – Principal stresses in the formation

In most cases it is good to assume that the principal stress directions are aligned with the vertical and horizontal axis x, y and z. These stresses are called:

- S_V (S1 in the cube): this is the vertical (overburden stress). The cube supports the weight of the formation above, and therefore is subject to a compressive stress.

- The horizontal stresses (S2 and S3 in the cube above). If you apply a compressive load to a cube of certain material, it will compress vertically and expand laterally, as predicted by its Poisson coefficient (ν). A cube of formation cannot expand freely as its neighboring cubes are also suffering the same compression from the overburden. Therefore, the cube will feel a horizontal stress of at least:

$$S_{2-3} = S_V \left(\frac{\nu}{1-\nu}\right)$$

  This calculation of the horizontal stress will be an absolute minimum, as in reality the tectonic stresses will impose a larger magnitude of the horizontal components. In general, we refer to:
  - S_{Hmax}: Maximum horizontal principal stress
  - S_{hmin}: Minimum horizontal principal stress

  When we perform a minifrac we can actually find the S_{hmin}, as the fracture will propagate perpendicular to the direction of the minimum value of the 3 principal stresses.

In reality, due to the poroelastic behavior of the rock, the effective stresses that the rock feels are also related to the formation (or pore) pressure, which counteracts the effect of the principal stresses. The effective stresses are calculated as:

$$S_{i_{eff}} = S_i - \alpha\, P_P$$

Where P_p is the formation (pore) pressure and α is the Biot cofficient.

So now we know that the stresses on the formation can change throughout the well's life. The formation pressure will change (depletion), which will modify the vertical and horizontal stresses. This becomes very clear in high compressibility rocks that exhibit subsidence. Different formation levels can also deplete at different rates, and then the effective horizontal stresses will vary with depth.

In formations where there is a large horizontal stresses contrast, ovalization can occur. A cross section of a cased well is shown in Figure 28, from where it can be seen that the S_{Hmax} acts in the direction of the IDmin arrow. Once the casing is effectively cemented in place, the stresses are transmitted from the borehole to the formation.

Finally, tectonic movements, typically along faults or bedding planes, can occur. This typically looks like shear movements of the casing, along the fault plane. This type of deformation may be very sudden.

6.2. Identifying deformation from MFC data

The MFC image (unwrapped fingers radii), diagnostic plots and statistics of processed MFC data of deformed pipes do not show any sign that something may be wrong. This has caused problems in the past, when the whole dataset was centralized blindly (or automatically by the acquisition system) and the interpreter missed some hints on the raw data and the calculated eccentricity.

The explanation will consider a case of planar shear, but this will be later extended to other types of deformation.

The image below shows the raw MFC image, diagnostic plot, Eccentricity, schematic on the MFC going through the deformed interval and cross sections.

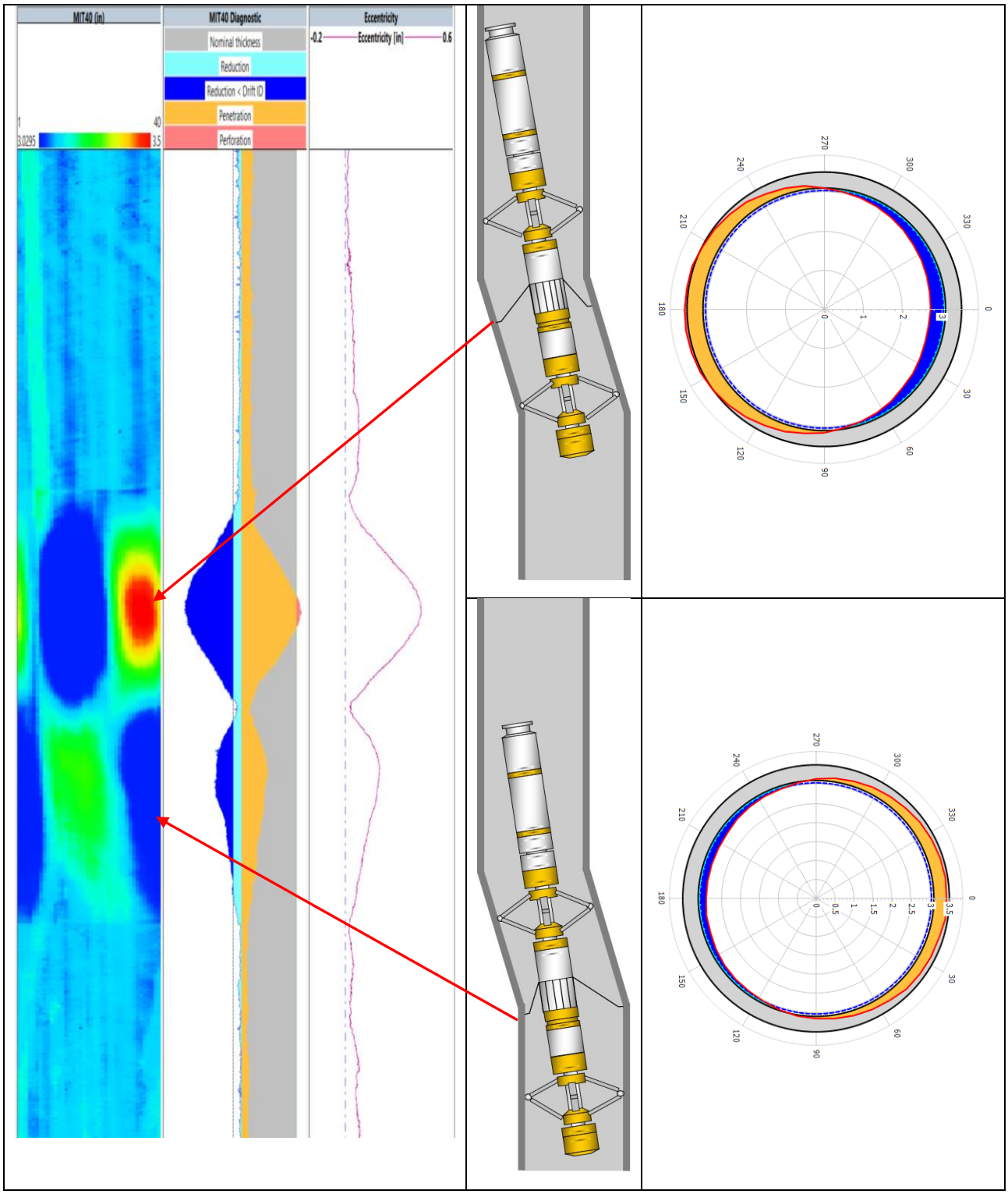

Fig. 36 – Shear deformation and MFC behavior

MFC tools are always run with centralizers above and below, and we will assume that these are perfectly centralized in the pipe and that the MFC tool is rigid. The measurements are described below, as the MFC moves from the bottom to the top of the interval:

1. Before the top centralizer reaches the deformed interval, the MFC has a 'baseline' eccentricity value (depending on the pipe deviation)
2. As the top centralizer enters in the deformed region (lower bend) but remains centred in the pipe, the MFC will start to experience an increased eccentricity, as the tool centre moves to the side (closer to the bend). The eccentricity will reach a maximum when the fingers are at the bend itself.
3. When both centralizers (and therefore the MFC) are in the deformed section, the tool will be parallel to the (deformed) well trajectory. The eccentricity will be back to a baseline value.
4. As the top centralizer reaches the end of the deformed interval (upper bend), the MFC will again start to increase its eccentricity, but compared to the bottom bend, the eccentricity direction will be opposite, for a case of planar deformation. Again, the maximum eccentricity will be reached when the MFC is exactly at the bend depth.
5. As the tool continues moving up, the eccentricity will decrease until the bottom centralizer leaves the deformation (lower bend), where the eccentricity will return to the baseline.

From this analysis, it is possible to conclude that the MD distance between the eccentricity peaks maxima corresponds to the deformed distance. Using the value and the direction of the eccentricity, and with the knowledge of the geometry of the toolstring dimensions, it is possible to estimate the trajectory changes in 3D. This can be used to understand the severity of the deformation, and assess whether it will be possible to re-enter the well with certain tool or pipe diameter.

The Figure below shows the same interval after centralization. Apart from the high eccentricity value, there is no evidence whatsoever in the images or the statistics, that this interval of the well may be deformed. This stresses the need for a thorough QAQC of the raw data, before jumping into the MFC processing options.

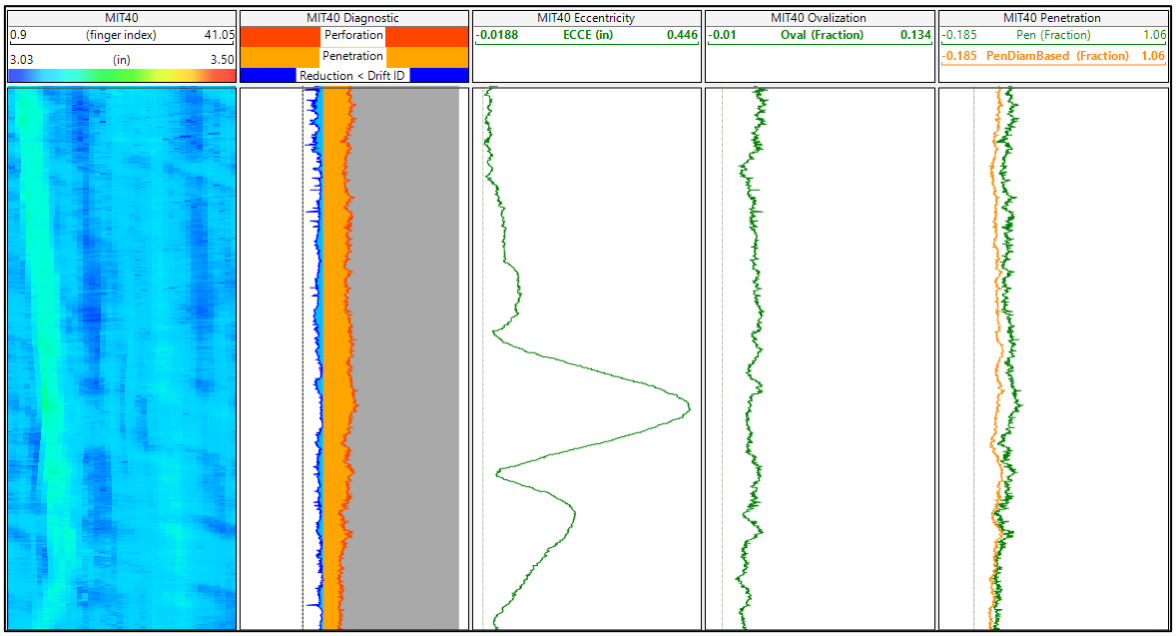

Fig. 37 – Centralized deformed interval

6.3. Other types of deformation

Apart from ovalization and shear, there are other typical deformation behaviors that can be diagnosed by MFC. For shear we saw that two peaks on the eccentricity (with opposite eccentricity direction) means the pipe moving laterally (in X, Y or both axis). The cases below include more than one lateral displacement, and therefore more eccentricity peaks. The same explanation presented above can be extrapolated to the following scenarios:

Bending

Adding an extra peak on the eccentricity and again changing the eccentricity direction would be a case of a bend, as shown below. This failure type can represent a serious well access problem when the bend occurs over a short distance, as the tortuosity will increase. This image also shows the radius track, which is a must for diagnosing any type of deformation, due to the very characteristic shape and clear indications of eccentricity change in both magnitude and direction.

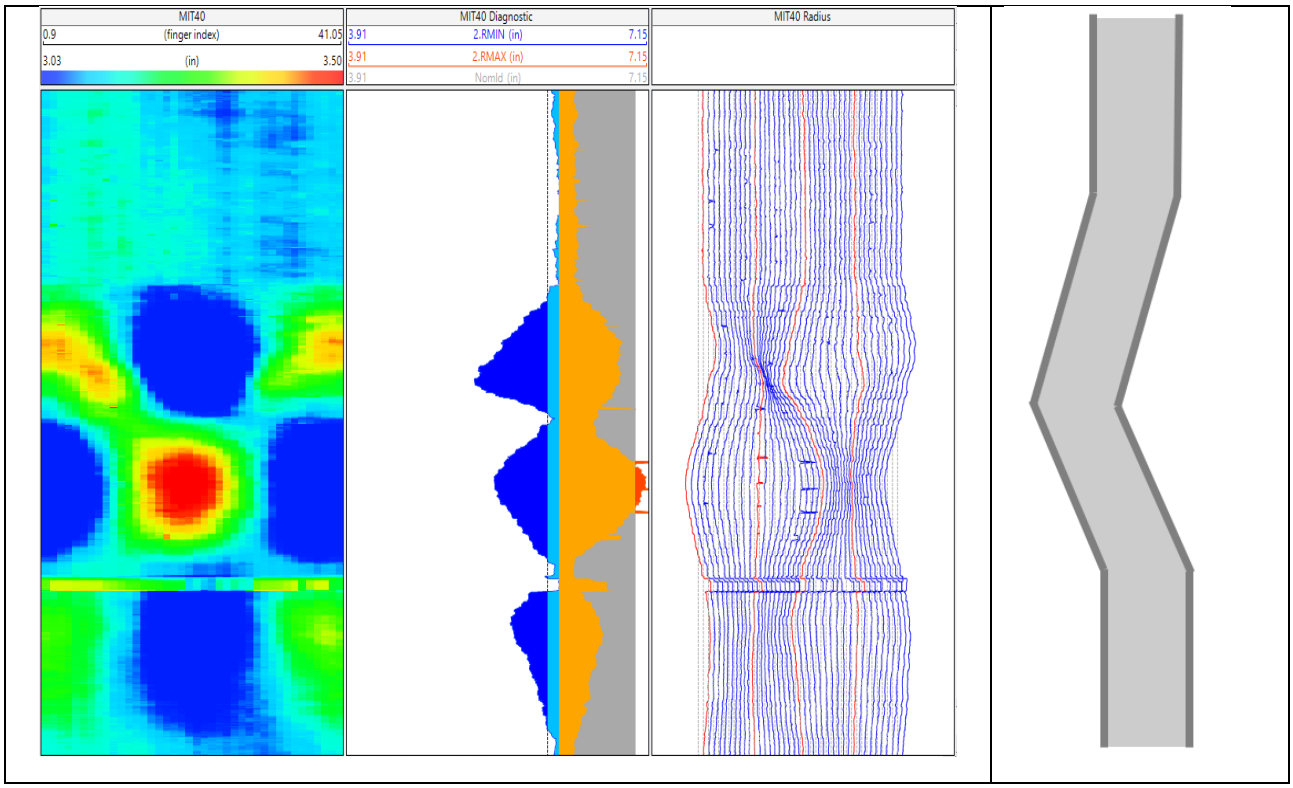

Fig. 38 – Bend on a casing

Buckling

Axial loads in the pipe can be caused by the weight of the different completion components, thermal expansion, pressure loads, etc. If these loads are high enough, the casing or tubing can deform and reach another stable configuration inside the borehole or the pipe which contains it. This new configuration can be S-shaped (typical in coiled tubing operations) or helical.

The image below shows a typical case of helical buckling. The eccentricity track shows 6 peaks, meaning that there are 5 intervals where the pipe changes trajectory due to deformation.

However, compared to previous cases, it can be seen that the eccentricity direction does not change 180 degrees for every peak, but changes continuously, in this case clockwise (from bottom to top). This is a clear case of a pipe with a corkscrew shape. The radius track is again a key QC plot for assessing deformation.

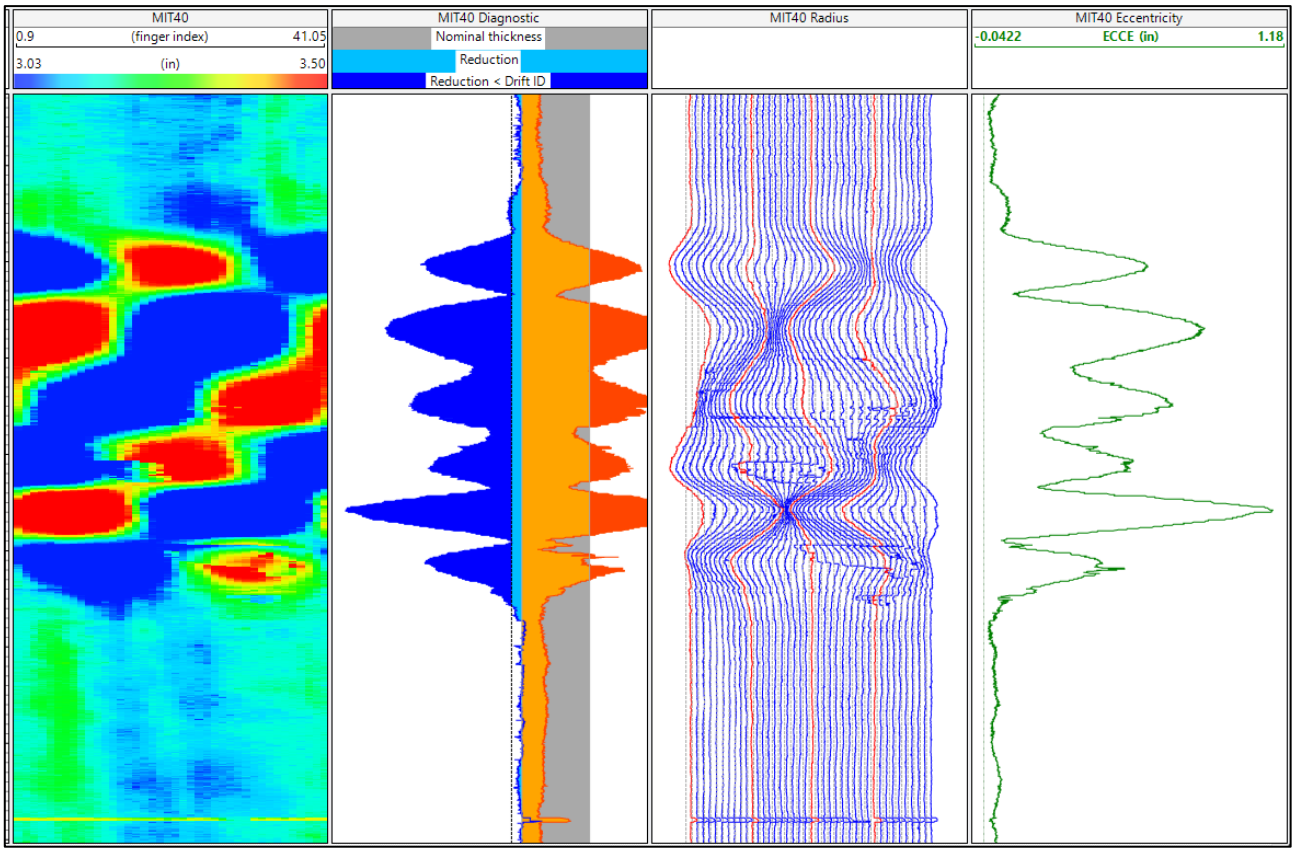

Fig. 39 – Helical buckling

In any case, locating the deformation and understanding the severity of the tortuosity are key aspects on the design of future well interventions. An extreme deformation may impede the possibility or re-entering the well, with severe consequences on its production performance and ultimately the design of P&A.

7. Ultrasonic tools

A different technology for determining the internal pipe radius consists on measuring the transit time of an ultrasonic pulse, while a rotating head sweeps the internal circumference. This family of tools, generically known as Pulse-Echo or Acoustic Televiewers, is also used for other applications, including open hole (borehole) images, pipe thickness and cement evaluation. In this document we will focus on the determination of the internal radius and its processing.

The typical field deliverables include a calculation of the pipe internal radius and derived statistics, based on the processing of the transit time. Like MFCs, these tools also suffer from eccentricity, and therefore in order to obtain a representative radius map it is necessary to centralize the data. The implications of a poor or an automatic centralization were explained in

the previous sections, and these are equally applicable to ultrasonic tools. Therefore, the objectives of this section are for the user to be able to understand the steps to go from the raw to processed data, to be able to QC the field product, and if necessary to recompute the internal radius and obtain the statistics from scratch.

7.1. Measurement principle

The most typical ultrasonic tools contain a rotating sub, which spins several times per second (5-8 times per second). While rotating it emits high frequency ultrasonic pulses (typically higher than 150 kHz). The same transducer that generates the pulse also measures the returns of the acoustic waves, which reveal different characteristics of the materials that the pulse encounters (fluid, pipe, cement, formation).

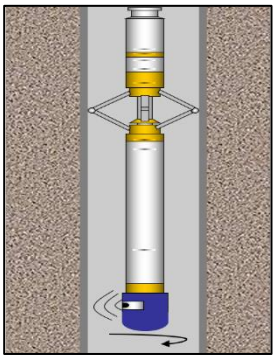

Fig. 40 – Schematic of ultrasonic tool

The ultrasonic pulse will travel through the borehole fluid (mud, water, oil, etc.) at certain velocity. When it reaches the first interface (pipe), part of the energy will be reflected, and part will be transmitted to the pipe, where it will travel at a different velocity. The amount of energy that will be reflected and transmitted is a function of the material's acoustic impedance (Z), given by the density multiplied by the velocity. The acoustic impedance has units of Rayleigh, typically abbreviated MRayl. For planar waves, the Reflection (R) and Transmission (T) coefficients, are given by:

$$R = \frac{(Z_2 - Z_1)}{(Z_2 + Z_1)} \qquad T = \frac{2\,Z_2}{(Z_2 + Z_1)}$$

It is the first reflection at the pipe wall that will contain the information about the distance from the transducer to the pipe. However, the fraction of the acoustic wave that is transmitted to the pipe will also find another interface, typically a cement or the fluid that remained between the pipe and the formation. Therefore, more transmissions and reflections will occur, with the soundwave bouncing back and forth between the pipe ID and OD.

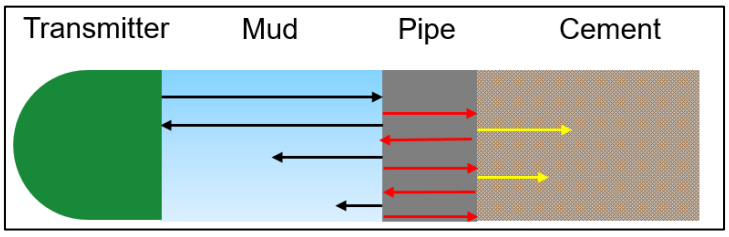

Fig. 41 – Acoustic interactions with the different materials

The subsequent arrivals to the transducer will contain information about the pipe thickness and the cement impedance. This analysis is done in the frequency domain. However, as mentioned previously, we will focus on the determination of the internal radius, which is done in the time domain through the transit time of the first return.

The tool is configured to emit a number of pulses per rotation (18, 46, 72, etc.). For each pulse, the tool will record the returning waveform. As shown in the image below, for each angle or 'azimuth' a VDL plot is presented, from where it is possible to analyze the waveform at any depth. The transit time, from the pulse firing to the return of the pipe bounce, is presented for one depth. Repeating this process for every depth and all the angles, a transit time map is exported.

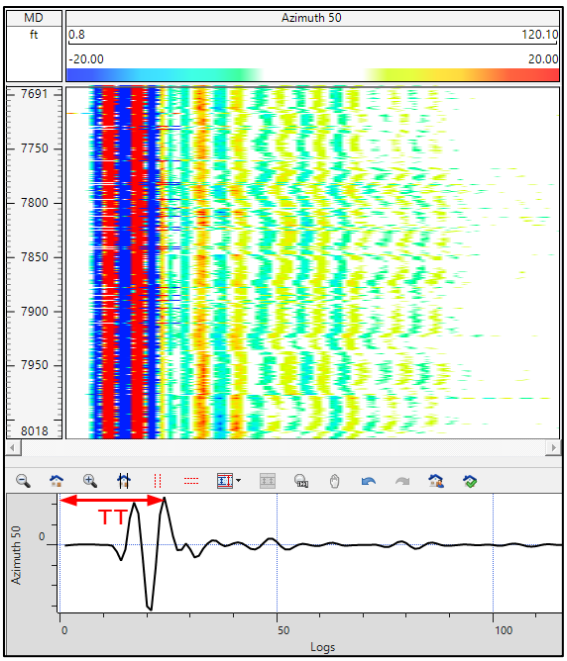

Fig. 42 – Waveform VDL for one angle

7.2. Internal radius from transit time

The transit time (u-sec) for the different azimuths is presented as an array image, as shown below. Displaying the measurements at different depth it is clear that the measurements are eccentric, as we have seen for the MFC. However, before worrying about the centralization we need to move from time to length.

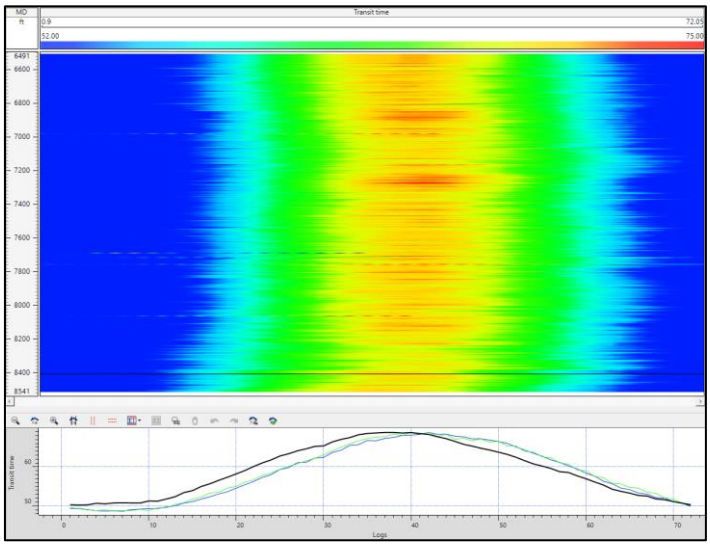

Fig. 43 – Transit time map

The acoustic velocity and impedance of the borehole fluid varies with depth, pressure and temperature. Since the different output of the ultrasonic tools rely on these parameters, it would not be accurate enough to use correlations for predicting the downhole values. Instead, in-situ fluid properties measurements of impedance and density are recorded by the tool. At different depths, the properties of the fluid between the transduced and a target plate (inside the tool sub) are measured.

With the knowledge of the fluid velocity (FV), also expressed as 'fluid slowness' (inverse velocity), the internal radius can be calculated as:

$$IR_{TT} = \frac{TT}{2} * FV + Offset$$

The offset accounts for the fact that the transducer is not exactly at r=0 in the tool, but the emitter/receiver is at certain distance from the tool centre. This depends on the sub type, as there are various sizes depending on the ID to be measured. In Emeraude, the internal radius can be computed from the transit time using the 'ab' option.

The transit time is shown next to the Internal radius images and the MFC diagnostic plot. The next step is centralization, and should be done with the considerations explained in Section 3.1.

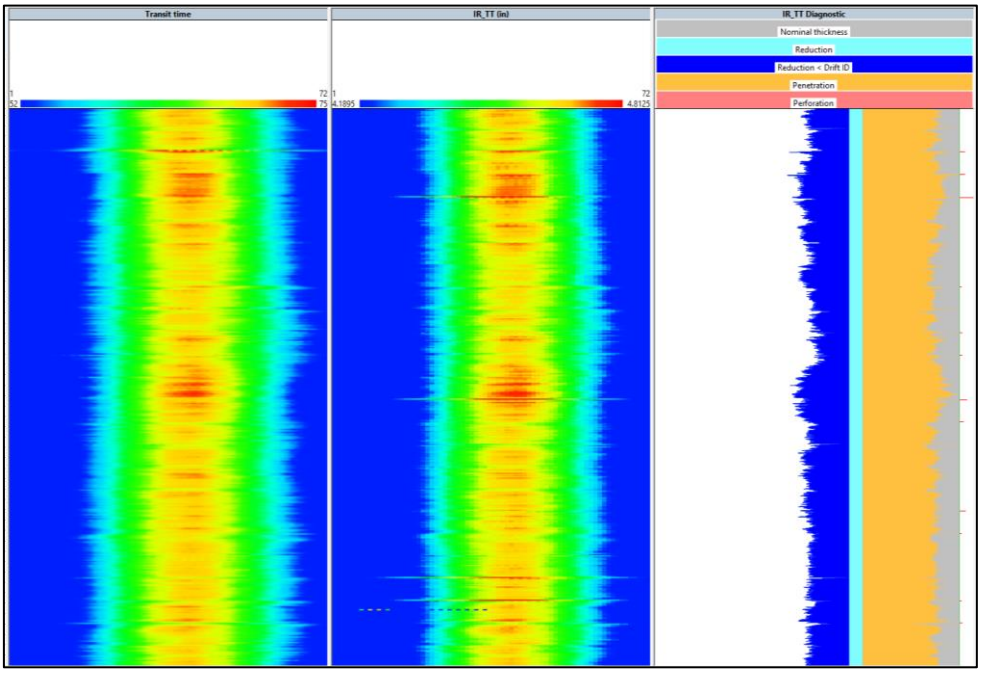

Fig. 44 – Transit time, Internal radius and Diagnostic track.

7.3. Final results

After centralizing the transit time-derived internal radius data, the statistics per joint can be computed and the final results can be extracted. It should not be necessary to apply any other editing, unless there are clear telemetry or electronic noise. The results are shown in the image below. With the knowledge that this log was run as part of a cement evaluation job, during the well construction stage, one would expect the internal radius to be similar to the nominal, or at least within tolerance. As seen in the image below, the penetration is larger than 20% in most joints (yellow color coding).

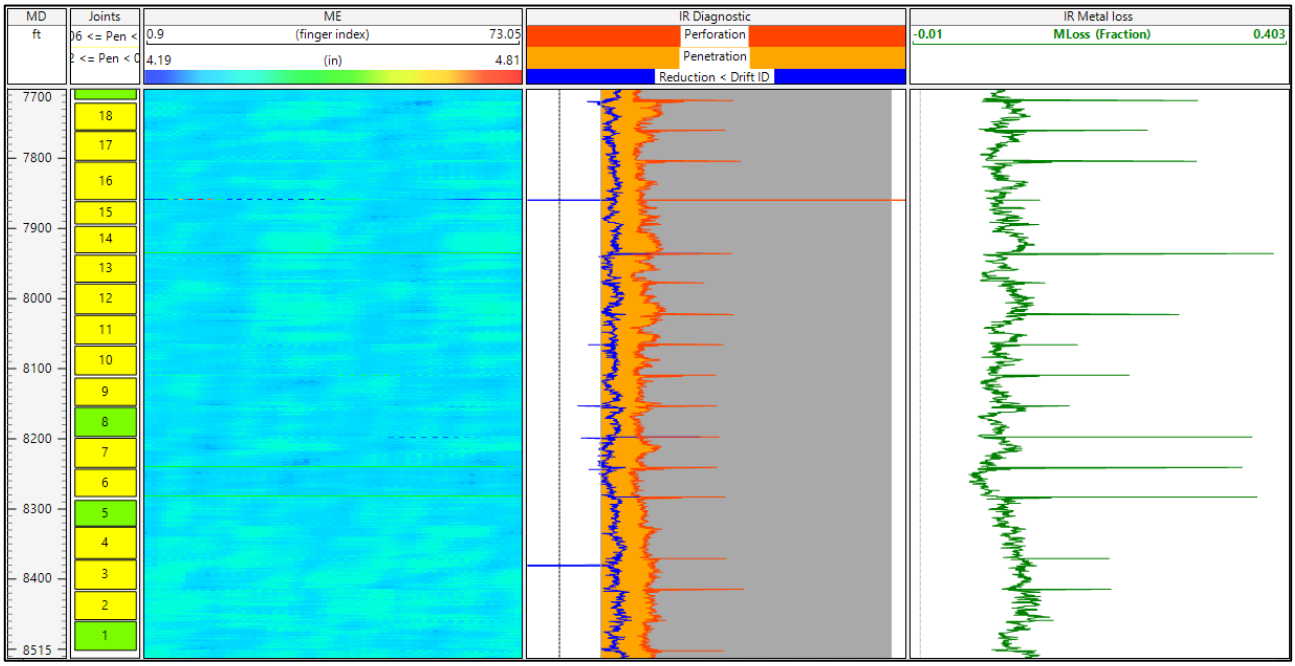

Fig. 45 – Final results from Ultrasonic radius measurement

An error on the internal radius calculation from transit time can be caused by three things (apart from tool failure):

- Transit time errors: can be related to the gating and should be fixed by re-setting the gates on the acquisition system
- Offset: If the radii values were calculated using a wrong tool geometry definition, then these will show a consistent larger or smaller value than the actual pipe
- Fluid velocity: The value used for computation may not be representative due to wrong bad measurements or different conditions (pressure, temperature, density)

The first step is to try to identify the source of the discrepancy. If this is due to a wrong fluid velocity, it is possible to apply the Recalibrate option in Emeraude, where a known ID can be used to compare the radius computations and, if necessary, apply shifts to the different radius computations.

Table of contents